Friction Surfacing Deposition by Consumable Tools

Ebrahim Seidi
Department of Mechanical Engineering,
University of Hawaii at Manoa,
Honolulu, HI 96822
e-mail: seidi@hawaii.edu

Scott F. Miller[1]
Department of Mechanical Engineering,
University of Hawaii at Manoa,
Honolulu, HI 96822
e-mail: scott20@hawaii.edu

Blair E. Carlson
General Motors Tech Center,
Warren, MI 48092
e-mail: blair.carlson@gm.com

Friction surfacing is a new variation of friction stir processing for surface property modification of metallic substrates. There is an increasing body of literature about friction surfacing by deposition of metal from a consumable tool to a solid substrate. Friction surfacing has many potential applications in joining, coating for corrosion resistance, and repair of degraded components. This article presents a review of the basic principles and latest research organized by processing techniques and variations, thermomechanical transfer and deposition of material, and finally metallurgical, mechanical, and chemical properties of the resulting deposition. Different friction surfacing processes are reviewed of novel tool–substrate configurations for material deposition for noncoating purposes like keyhole filling and joining dissimilar materials. Possible future topics of study for this area are discussed, which include deeper understanding of material transfer through metallurgy, FEM, and scale up of the technique for practical application.
[DOI: 10.1115/1.4050924]

Keywords: additive manufacturing, coating, solid-state deposition, process parameters, characterization, mechanical properties

1 Introduction

Friction surfacing is a thermomechanical solid-state technique that can be used to deposit metal from one surface to another. This is an emerging field of joining and coating technology as compared to more conventional fusion techniques, as shown by Cai et al. [1]. As shown in Fig. 1, friction surfacing is one of the applications of friction-based techniques, invented by Klopstock and Neelands [2]. Friction surfacing creates a solid-state deposition by employing a rotating tool that is forced onto the surface of a workpiece along its axis. Frictional heat is then generated from the high force between the rotating tool and workpiece. Once the temperature at the tool–substrate interface sufficiently elevated (~3/4 melting temperature) and the consumable material softened, the tool is moved across the substrate surface. Consumable material is stirred and transported by the tool onto the substrate surface, facilitating the solid-state deposition. This technique produces high-quality deposits suitable for a broad range of tool–substrate materials [3].

The applications of friction-based techniques are friction welding, friction drilling, friction forming, and friction surfacing, as shown in Fig. 1. These are thermomechanical processes that combine high force and frictional heating for different applications. There have been reviews about friction welding [4–9], friction drilling [10], and friction surfacing in general [3]. Friction stir surface modification by friction surfacing has also been reviewed [11–14], but what is lacking is a review of the literature on the friction surfacing process using consumable tools. Gandra et al. [3] published a thorough review of friction surfacing in 2014, but there have been new variations in processing techniques and applications recently. This article provides an updated review of the literature pertaining to material deposition by friction surfacing from a consumable tool. In Sec. 2, the literature is organized based on the various processing techniques. Section 3 is devoted to the characterization of thermomechanical transfer and structure of deposition. Section 4 presents a review of the metallurgical and mechanical properties of the deposition. Finally, in Sec. 5, research challenges, future trends, and recommendations are presented. Figure 2 shows a schematic of the friction surfacing process, specifically where the rotating tool is consumed by rubbing against the substrate and thereby the transferring material. A layer of consumable tool material is transferred from the tool to the substrate along the contact path of the tool across the substrate [16].

Friction surfacing makes it possible to create a thick, fine-grained, coating layer on the substrate for improving the mechanical properties. The heat energy is provided by frictional contact and shearing of material inside the tool adjacent to the tool–workpiece interface [17]. The internal shearing above the strain hardened viscoplastic layer of consumable tool material enables the transfer of material onto the substrate surface, as shown schematically in Fig. 3. The most significant generation of heat in this technique is from viscous shearing caused by friction between the remaining tool and transferred material from the tool, as was reported by Vilaça et al. [19]. Friction surfacing could be employed as an advanced surface modification approach; therefore, it is important to study the mechanisms that lead to material transfer in this technique. This will result in better control and quality of deposition.

There are various process parameters that impact the final results, including tool feed rate, rotation speed, normal contact force, and tilt angle have been studied as important process parameters by Liu et al. [20]. The deposition has been examined by hardness testing, image-processing approach, and optical microscopy. It has been proven by Gandra et al. that the tilt angle along the tool path can increase the deposition by as much as 5% [21]. Friction surfacing deposits material at a higher material transfer rate and lower specific energy usage than plasma arc welding, laser cladding, and other cladding processes.

The body of literature concerning friction surfacing has been growing in recent years and as shown in Fig. 4, and the number of publications and citations for this area of research has significantly increased in the past 20 years, becoming an increasingly important solid-state surfacing technique in the literature. This technique has many potential applications in the industry where deposition of metal onto a dissimilar material can be beneficial.

2 Friction Surfacing Processing Techniques

In this section, the literature is organized by the type of process: friction surfacing deposition from consumable rods, friction

[1]Corresponding author.

Manuscript received October 21, 2020; final manuscript received April 7, 2021; published online June 29, 2021. Assoc. Editor: Jingjing Li.

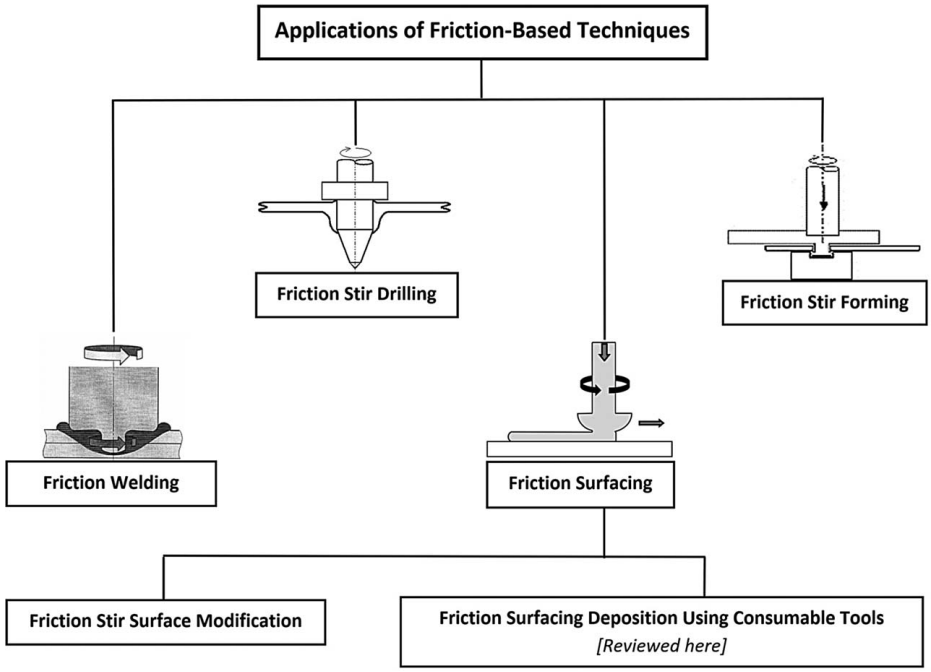

Fig. 1 Applications of friction-based techniques

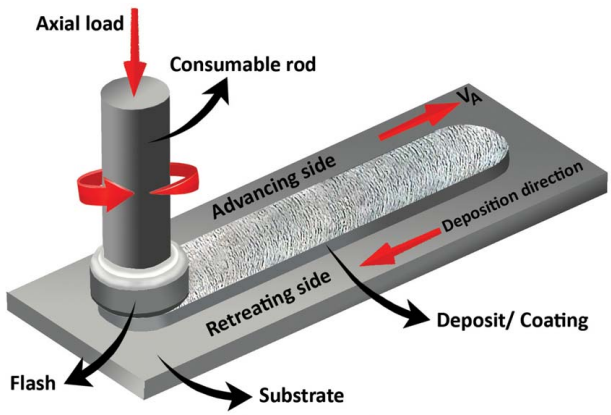

Fig. 2 Illustration of friction surfacing identifying the features and process parameters [15]

surfacing with reinforcing particles, and refill friction stir spot welding. Most of the research was focused on consumable rods, but the process has been altered depending on the application as reviewed in this section.

2.1 Friction Surfacing Using Consumable Rods With Varying Geometry and Material. Friction surfacing using a consumable rod is the most popular form of deposition as an alternative approach to fusion-based processes. Friction surfacing has been studied through many different processing techniques and variables for a variety of materials, as reported by the articles in this review. Table 1 lists the various combinations of tool–substrate materials and different processes that have been studied. To provide a better comparison, Fig. 5 presents the trend of consumable tool materials utilization in the investigation. From the table, it can be noted that steel and aluminum alloys have the highest frequency of being studied as both tool and substrate materials, and the

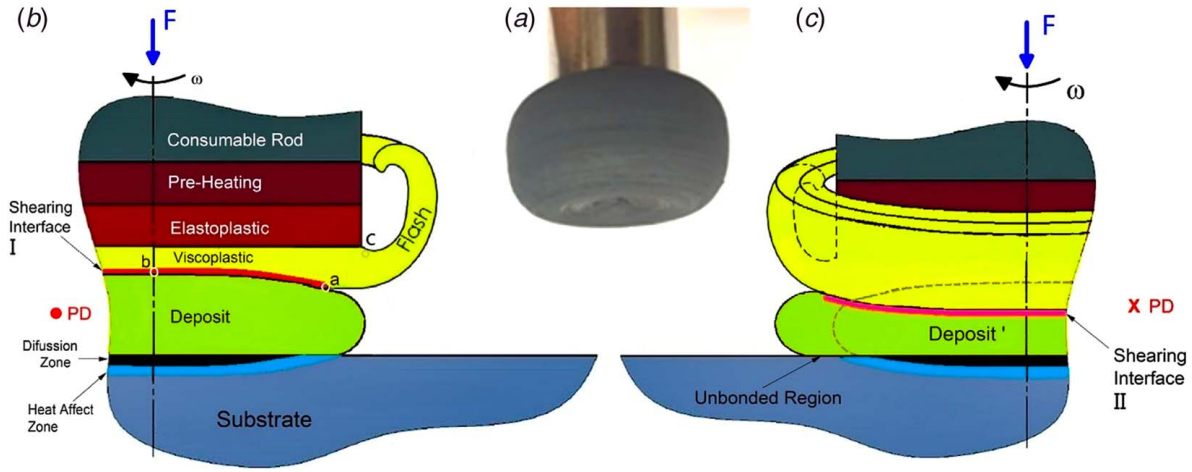

Fig. 3 (*a*) Consumable rod after friction surfacing process; schematic identifying different zones and coating formation mechanism observing from (*b*) process direction and (*c*) reverse process direction (*F*, axial force; *ω*, tool rotational speed) [18] (Reprinted with permission from Elsevier © 2019)

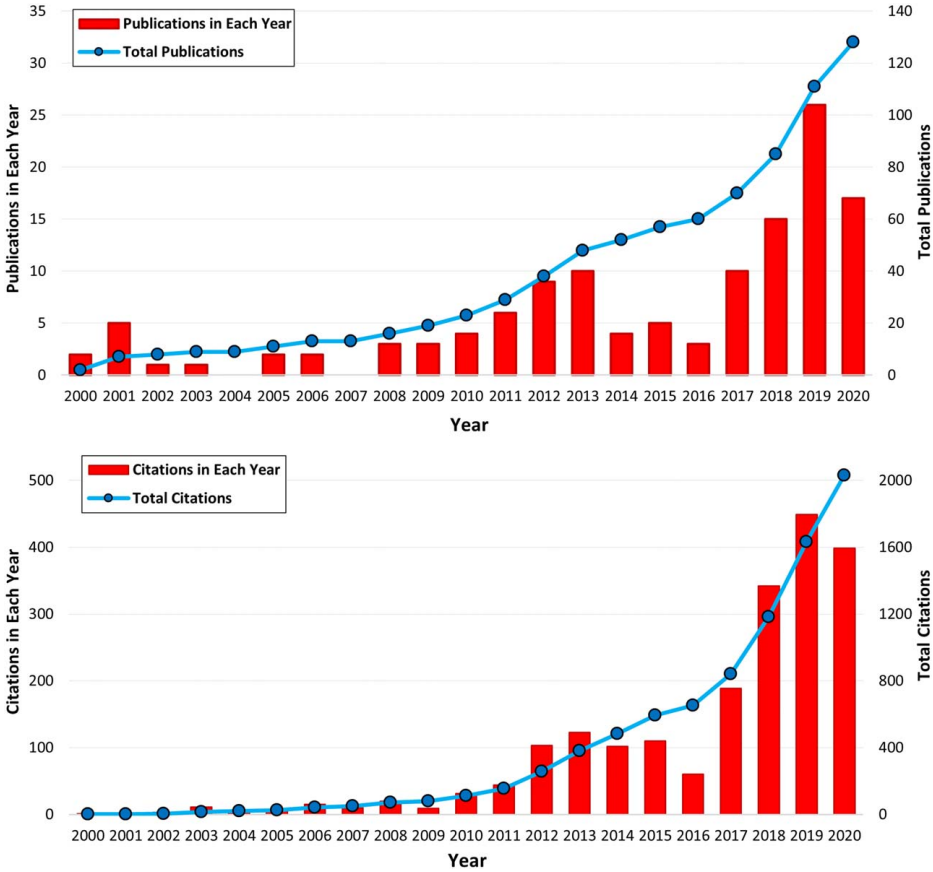

Fig. 4 Interest in the friction surfacing technique as measured by the number of published items (top) and number of citations (bottom), Created by the authors from an ISI Web of Science search with "friction surfacing" as "topic," Accessed March 8, 2021

consumable rod process is most common among the seven different processes.

The transfer of Stellite-6 onto a steel substrate by friction surfacing was compared to deposition of the same material by plasma transferred arc and gas tungsten arc welding processes using a cast rod by Rao et al. [129]. The friction surfacing coating layers were found to be harder and exhibited a finer and more uniform distribution of carbide particles compared to plasma arc and gas tungsten arc joining processes. The finer grain size of the coating highlights one advantage of friction surfaced materials.

Not all materials are suitable for deposition by friction surfacing, and much of the literature is focused on specific material combinations. Chandrasekaran et al. investigated the viability of friction surfacing mild steel, aluminum, stainless steel, Inconel, and titanium as the consumable rod material onto mild steel and aluminum [60]. Inconel, mild steel, and stainless steel were friction surfaced onto aluminum substrates successfully, but titanium deposition was not possible. The viability of friction surfacing an aluminum alloy 6351-T6 consumable tool onto a steel alloy substrate was investigated by Badheka and Badheka [61]. Friction surfacing was carried out using 8, 12, 16, and 22 mm diameter consumable tools applied to a steel substrate of 6 mm thickness. The feasibility of creating AA6351 coatings on a 1020 carbon steel substrate using friction surfacing technique was investigated by Da Silva et al. [62]. It was found that the heat generation during the process is sensitive to the initial substrate surface roughness. Gandra et al. employed the friction surfacing technique to deposit AA6082-T6 consumable rod on AA2024-T3 substrate [22]. In Fig. 6, the evolution of both force and torque applied to the consumable tool, and the displacement along the tool axial direction is presented. The consumable tool was pressed against the substrate with an axial load, resulting in a sharp increase in torque and force upon contact. Ehrich et al. studied friction surfacing of AA6060 aluminum with additions of 6.6, 10.4, and 14.6 wt% Si, and 2 and 3.5 wt% Mg onto AA2024 substrate [42]. They found that a higher Mg content in the consumable tool reduced the thermal softening rate. Increasing Si or Mg content in the AA6060 consumable rod resulted in decreasing deposition dimensions, with the larger effect measured for Mg addition.

The coating of stainless steel alloy onto spheroidal graphite iron by friction surfacing was investigated by Nixon and Mohanty [87]. The microstructure produced a strong bond between the ductile iron and the stainless steel with no visible cracks in the heat-affected zone (HAZ). Bending and corrosion tests yielded results that confirmed that friction surfacing is suitable for corrosion resistance of pumps for petrochemical vessels. The feasibility of friction surfacing of copper onto mild steel using different process factors has been examined by Jujare et al. [127]. An improved copper coating was produced on relatively rough surfaces fabricated by rough milling. As shown in Table 2, uniform and continuous coatings were formed only with a specific combination of rotational and scan speed, and their quality varied according to the frictional heat developed between the tool and the substrate. Kramer de Macedo et al. studied deposition layers of three different tool materials (AISI 310, ABNT 4140, and ABNT 8620 steel tool) surfaced onto ABNT 1070 carbon steel [88]. They proved that friction surfacing can be used to repair the surface of high carbon steel and produce deposition on steel alloys. The repair of aged structural elements in nuclear plants by friction surfacing has been investigated by Yamashita and Fujita [133]. Stegmüller et al. studied friction surfacing of an EN AW6060 aluminum alloy using an austenitic stainless steel AISI304 consumable rod supplemented by an inductive

Table 1 Material combinations and process variations of friction surfacing

Tool material	Substrate material	Tool feeding method	References
Aluminum	Aluminum	Consumable rod	[22–41]
	Aluminum	Reinforcing particles	[42–52]
	Titanium	Reinforcing particles	[53]
	Aluminum	PMAFS	[54]
	Aluminum	RFSSW	[55–58]
	Copper	Filling friction stir welding (bit)	[59]
	Steel	Consumable rod	[15,60–79]
	Steel	Spot welding (bit)	[80,81]
Steel	Aluminum	Consumable rod	[82–86]
	Steel	Consumable rod	[18–21,60,74,78,87–114]
	Steel	Reinforcing particles	[115–117]
	Steel	Spot welding (bit)	[80]
	Copper	Consumable rod	[83]
Titanium	Steel	Consumable rod	[60]
	Titanium/aluminum	FS-HFSW	[118]
	Titanium	Consumable rod	[119–122]
	Titanium	Reinforcing particles	[123]
Brass	Steel	Consumable rod	[74]
Inconel	Steel	Consumable rod	[60,124]
Zinc	Aluminum	Consumable rod	[125]
	Aluminum	RFSSW	[126]
	Steel	Consumable rod	[125]
Copper	Copper	Consumable rod	[83,90]
	Steel	Consumable rod	[90,127]
Monel	Steel	Consumable rod	[128]
Stellite6	Steel	Consumable rod	[129]
NiAl-bronze	Steel	Consumable rod	[130]
Chromium–nickel	Chromium–nickel	Consumable rod	[131]
Magnesium	Magnesium	Consumable rod	[132]

Note: FS-HFSW, friction surfacing-assisted hybrid friction stir welding; RFSSW, refill friction stir spot welding; PMAFS, powder metallurgy-assisted friction surfacing.

heating process [82]. This investigation studied the deposition–substrate interface wherein an image recognition software tool was utilized to generate the interfacial roughness profile graph.

Shariq et al. examined the possibility of friction surfacing with different combinations of consumable rods and substrates by application of a conventional universal milling machine FNU2213 [83]. Commercially pure (CP) copper and AISI 304 were friction surfaced onto copper, mild steel, AISI 304, and AA1050 substrate materials. Friction surfacing stainless steel rod material onto the substrate of CP copper and CP copper onto CP copper were not successful. During the friction surfacing of CP copper onto CP copper, the copper could not tolerate a high temperature. Therefore, an

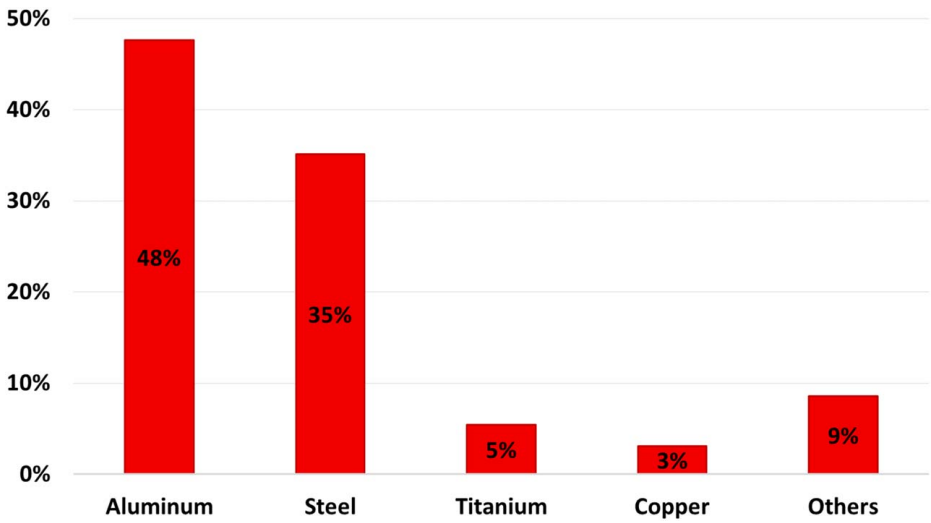

Fig. 5 Trend of consumable tool materials utilization in friction surfacing using consumable tools

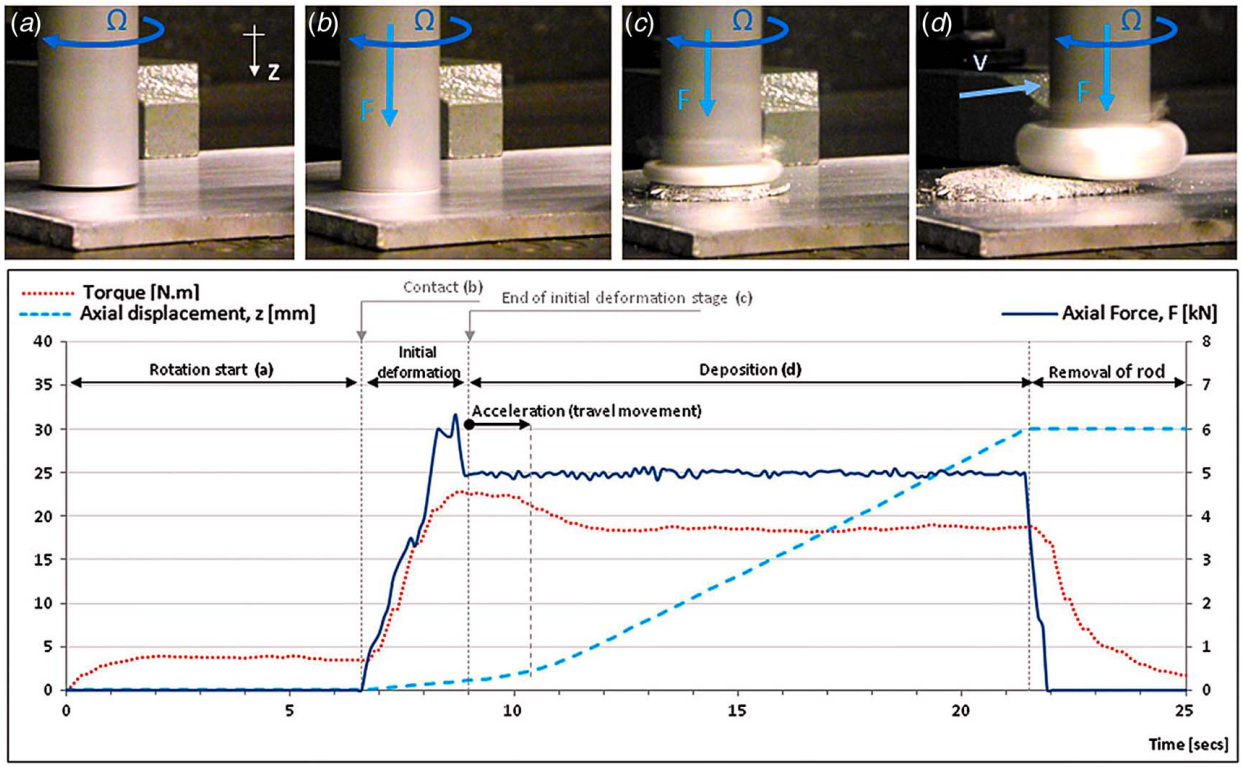

Fig. 6 Monitoring of torque, axial force, and displacement in the friction surfacing of AA6082 over AA2024: (*a*) rotation start, (*b*) initial contact, (*c*) end of initial deformation stage, and (*d*) deposition stage. Process parameters: axial force (F) = 5 kN, rotation speed (Ω) = 3000 rpm, travel speed (v) = 7.5 mm/s [22] (Reprinted with permission from Elsevier © 2013)

Table 2 Feasibility of friction surfacing deposition using different process parameters [127]

Sample No.	Force (kN)	N (rpm)	Scan speed (mm/min)	Comment	Acceptance
A	2	1250	20	Continuous, uniform width, satisfactory deposition	Yes
B	2	1500	20	Continuous, gradually increasing in width	Yes
C	2	1750	20	Discontinuous, nonuniform, and shearing deposition	No
D	2	1250	30	Uniform and narrow deposition	Yes
E	2	1500	30	Continuous and good deposition, but width is a slightly less than B	Yes
F	2	1750	30	Continuous good deposition, varying width	Yes
G	2	1250	40	Nonuniform, varying width, and shearing deposition at the end	No
H	2	1500	40	Nonuniform, continuous deposition	No
I	2	1750	40	Nonuniform, discontinuous deposition	No

optimized set of process parameters was required to create a balance between the mechanical stability and the maximum possible temperature that copper can withstand during the process, 974 °C. Although no bonding formation happened between the interface of the consumable rod and the substrate, a small amount of material flowed from the substrate to the consumable rod and was deposited onto the tool, which is unusual. To friction surface AISI 304 onto AA1050 substrate, a frictional heat-up plate of mild steel with the same thickness was welded to the aluminum substrate. The consumable tool was frictionally heated over the surface of the start-up plate until sufficiently plasticized, so that it could successfully be deposited onto the aluminum alloy substrate as presented in Fig. 7. Friction surfacing AISI 304 stainless steel onto AA1050 resulted in successful deposition with the mild steel heat-up plate method. The maximum temperature measured was 1415 °C.

Troysi et al. assessed the feasibility of AISI 304 stainless steel deposition onto AISI 1020 steel substrate [89]. The effects of parameters (substrate surface roughness, tool rotational speed, and traverse speed) on coating properties (geometry thickness and width, microstructure, microhardness, and push-off strength) were quantified. It was found that the substrate surface roughness did not have a strong effect on the deposition geometry; however, lower substrate roughness resulted in higher push-off strength. Thermal control is important for successful deposition in friction surfacing with consumable tools.

Rao et al. measured the thermal profiles produced by the different tool–substrate material combinations including steel/steel, copper/copper, and copper/steel [90]. Thermal profiles were recorded by infrared thermography during the process. Liu et al. modeled the temperature distribution in consumable tools for friction surfacing

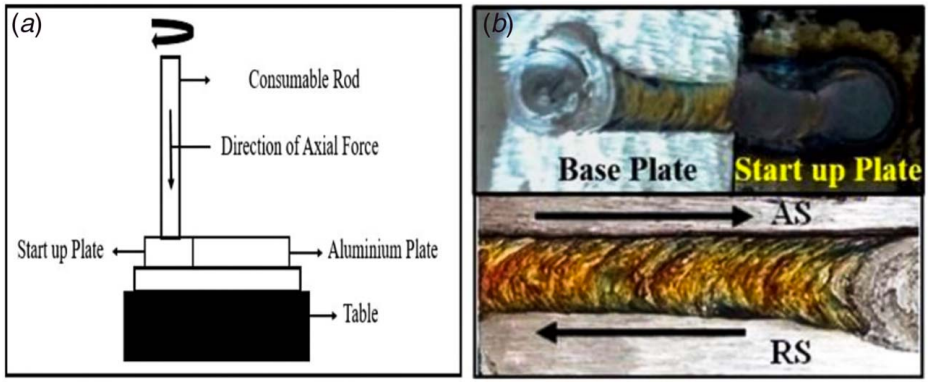

Fig. 7 (*a*) Illustration of the experimental setup and (*b*) friction surfacing of stainless steel onto aluminum workpiece with the heat-up plate method [83] (Creative Commons Attribution NonCommercial-NoDerivaties 4.0 International CC-BY-NC-ND 4.0)

with the applied finite difference method [134]. As shown in Fig. 8, the model output was consistent with experimental results and provided theoretical guidelines for technical parameters. Liu et al. also conducted a thermal analysis for friction surfacing 1Cr18Ni9Ti (321) rod onto the substrate of 1020 steel. The temperature was measured by a thermocouple at points of interest on the tool. There was a high change in temperature at the tool–workpiece interface at the beginning of the process. Once the frictional contact conditions reached the quasi-steady state, temperature change gradually decreased and became stable near the melting point of the tool material [91].

Sahoo et al. investigated the influence of different tool shapes in friction surfacing of A6063 tool with 100 mm length and 18 mm diameter onto IS2062 low carbon steel [63]. Five different configurations of the tools were chosen as presented in Fig. 9, entitled as mechtrode face 1–5 designed as follows: MF1 was a simple rod with a conventional flat surface at the tip of the rod, MF2 had a drilled hole with 10 mm length and 2 mm diameter at the center, MF3 had three holes with 10 mm length and 2 mm diameter (located triangularly), MF4 had a drilled hole with 10 mm depth and depth and 8 mm diameter, and MF5 had a tapered tip with 10 mm height and 8 mm diameter.

Friction surfacing falls in the category of friction-based additive manufacturing approaches [135]. Friction surfacing technology has been employed as a prospective additive manufacturing technique. In this technique, the rotating consumable rod deposits the first layer of the coating as it traverses along the substrate surface. In cases, where the size of the substrate is much larger than the rod diameter, multiple adjacent tracks are required to create the first layer of deposit on the entire substrate surface, as presented in Fig. 10. After depositing the first layer of the coating, it is subjected to a machining operation to provide a flat surface for the second layer of the coating. This process can be repeated by making a multilayer deposit until the desired build height is achieved [136,137]. Isupov et al. [23] investigated the single-layer and multilayer deposition and butt joint through the friction surfacing technique using Al–5Mg aluminum alloy for both tool and substrate material. Dilip et al. successfully employed the friction surfacing technique as an additive manufacturing approach [92]. In this technique, a multitrack multilayer deposit of mild steel consumable rod was fabricated to create a three-dimensional metallic part. The first, second, and third layers of this deposit consisted of five, four, and three tracks, respectively.

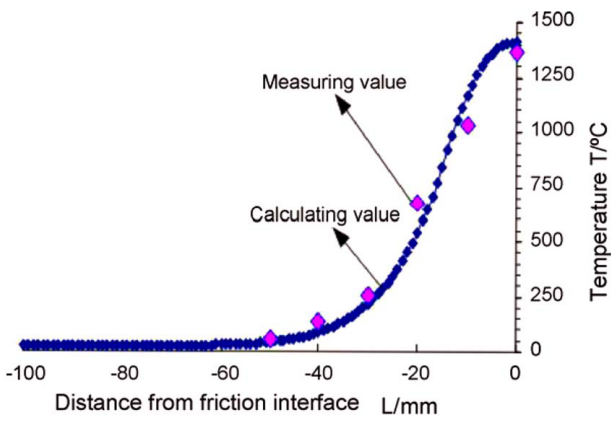

Fig. 8 Comparison of model output and experimental results for temperature (4000 N force; 1825 rpm spindle speed; time: 37 s) [134] (Reprinted with permission from Elsevier © 2009)

2.2 Friction Surfacing With Reinforcing Particles. In some applications, it is desired to apply a surfacing with reinforcing particles. Various methods are presented in the literature for incorporating the reinforcing particles within the consumable tool. A composite powder mixture of alloy and reinforcing particles can be pressed, or holes can be drilled along the length of the tool and then filled with reinforcing particles.

Single-layer and gradient deposition friction surfacing was investigated by Tosun et al. [24]. TiC particles were included to reinforce the AA7075 consumable tool, and AA 5754 was used as the substrate. The gradient deposition process consisted of a consumable rod fabricated by pressing a mixture of Al and TiC particles, and in this case, three overlapping layers at different reinforcement ratios with the outermost layer consisting of the highest particle content. The deposition with TiC particles resulted in significantly less wear, i.e., an improvement, compared to the powder-free depositions. Reddy et al. studied friction surfacing of 2124 aluminum alloy reinforced with silicon carbide (SiCp) particles (~30 μm in size) onto A356 aluminum [25]. They studied the corrosion and wear of the new material. The deposition was examined by metallography, dry sliding wear, and potentiodynamic polarization technique and was shown to be resistant to corrosion. Also, the deposition exhibited excellent metallurgical bonding and wear resistance (Fig. 11).

It was shown by Bararpour et al. that mechanical alloying can be accomplished in friction surfacing [43]. In this study, AA5083 and AA5052 aluminum alloys were used as the consumable rod and substrate materials, respectively, and Zn powder with 2.5 mm median size was filled into four holes in the consumable tool. The deposited samples had finer-grained microstructures than the A5083 consumable tool due to dynamic recrystallization (DRX) through the severe plastic deformation of a consumable material. The addition of Zn powder did not influence the general grain refinement of A5083. Bararpour et al. assessed the influence of

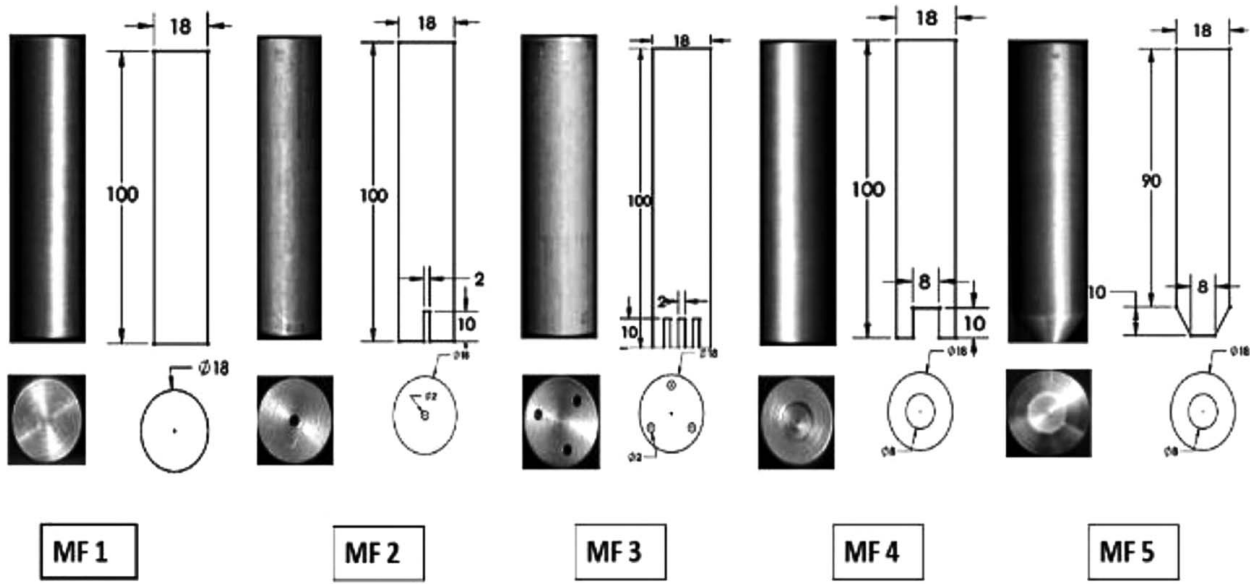

Fig. 9 The geometry and configuration of five different consumable tools [63]

nonisothermal aging on the mechanical properties and the microstructure of AA5083 with 15 wt% Zn composite deposition on A5052 substrate [44]. The zinc powder was inserted into four holes with a length of 30 mm and a diameter of 2.5 mm drilled in the tool. The highest hardness value and the ultimate shear strength of the composite deposition occurred at 185 °C. Due to the severe plastic deformation during the process, the particles became polygonal or round. In a similar approach, Bararpour et al. studied the effect of the zinc powder on the mechanical properties and the microstructure of Al-Mg alloy onto A5052 substrate [45]. The zinc powder was inserted into drilled holes in the Al-Mg aluminum alloy tool cross section. The Zn powder significantly increased the thermal stability of the deposition and decreased kinetic grain growth. The grain growth rate in the Zn-free and Zn-rich depositions was found to be 1.46 μm/h and 0.55 μm/h, considering a linear association between the heat treatment time and the grain size.

The friction surfacing of 6351-T6 aluminum alloy consumable tool with 22 mm diameter and SA 516 Gr 70 steel substrate with 6 mm plate thickness was studied by Badheka and Badheka [64]. Single-layer friction deposition was completed using consumable tools with and without additions of boron carbide particles. A triangular drilling hole pattern with 50–55 mm depth was selected, and the boron carbide powder in the range of 8–12 μm was inserted into the aluminum consumable tool. It was observed that adding B_4C particles increased the deposition hardness; however, it is very important how the particles were spread on the coating layer. Moreover, adding boron carbide particles results in the improvement of wear resistance.

Stainless steel 316L/TiB_2 material was successfully friction surfaced onto stainless steel 304 substrate by Guo et al. [115]. Blind holes were drilled in the cylindrical 316L tools to hold TiB2 powder reinforcement to be added in the process. In another investigation by Pirhayati and Aval [26], AA2024-Ag composite

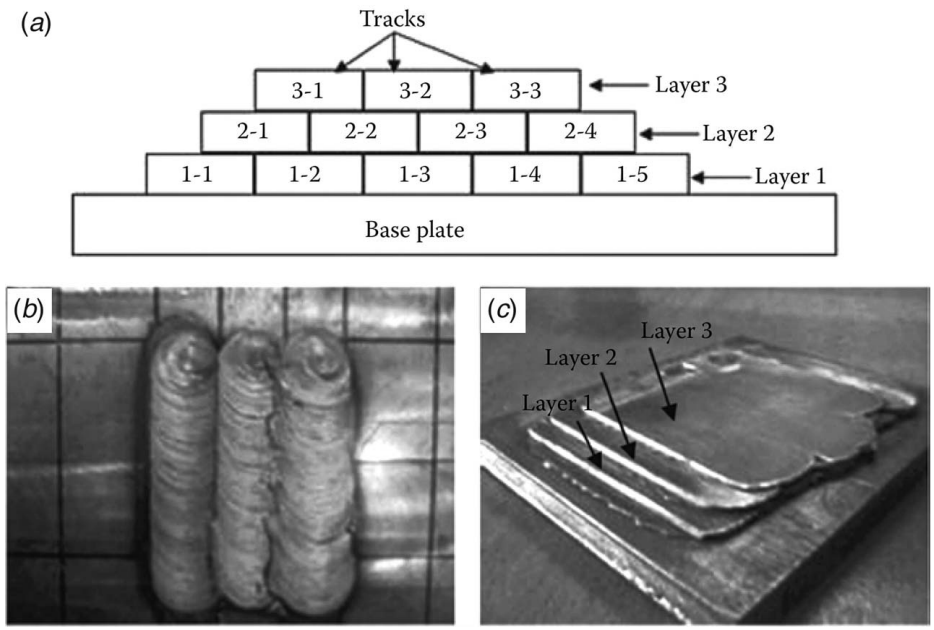

Fig. 10 (*a*) Schematic illustration of layers and track in friction surfacing of three layers, (*b*) three deposited tracks in the first layer, and (*c*) multilayer friction surfaced deposit [136]

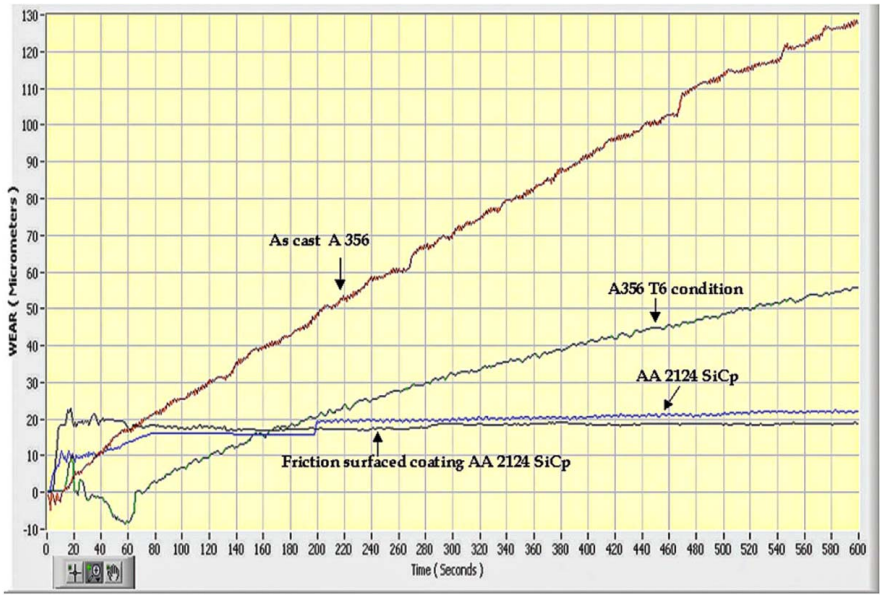

Fig. 11 A comparison of wear behavior of the materials [25] (Reprinted with permission from Taylor & Francis © 2009)

consumable rod was prepared by drilling three holes of a diameter of 2.5 mm and a length of 30 mm in the tool and filling them with silver particles with an average size of 1.55 ± 0.45 μm. The composite consumable rod was used to produce deposition onto the surface of the AA2024 substrate. The silver particles inserted into the consumable rod improved the thermal stability of the deposition. Oliveira et al. investigated 6351-T6 aluminum alloy deposition onto the substrate of AA5052-H32, reinforced with Al_2O_3 particles [46]. Holes were drilled in the consumable tool that was filled with the Al_2O_3 particles. The incorporation of Al_2O_3 particles resulted in greater hardness values of the deposited layer.

Pirhayati and Aval [27] also evaluated the possibility and influence of postheat treatment on friction surfacing of A2024 with 16 wt% Ag composite coating on the A2024 substrate. The addition of Ag powder did not positively influence the deposition's recrystallization behavior; however, it resulted in finer microstructures mainly due to the solid solution and lower frictional heat generated during the process. Moreover, the strength and surface hardness of Ag-containing coatings were higher than Ag-free coatings. In another recent investigation [47], they made three different consumable rods by adding 5.3, 10.6, and 16.0 wt% of Ag into the drilled holes into the cross section of an AA2024 consumable rod. The holes had the same depth and the diameter of 80 mm and 2.5 mm, respectively. In all these three configurations, the hole center was 3 mm away from the tool center. In the two-hole and three-hole configurations, the holes were at an angle of 180 deg and 120 deg with respect to each other, respectively. The Ag powder decreased the coating efficiency during the friction surfacing of the AA2024 aluminum rod. By considering a linear relation, it can be noted that by increasing 1 wt% Ag, the hardness and strength of the deposits increased by 1.0% and 1.8%, respectively; however, the electrical conductivity reduced by 0.12% International Annealed Copper Standard (IACS).

Miranda et al. investigated the creation of functionally graded material (FGM) composites using SiC and alumina reinforcement particles through the friction surfacing technique [48]. In another investigation, the friction deposition approach was successfully applied to create an aluminum matrix composite reinforced with titanium particles. As demonstrated in the schematic diagram of Fig. 12, the result was a deposition of the multilayer composite

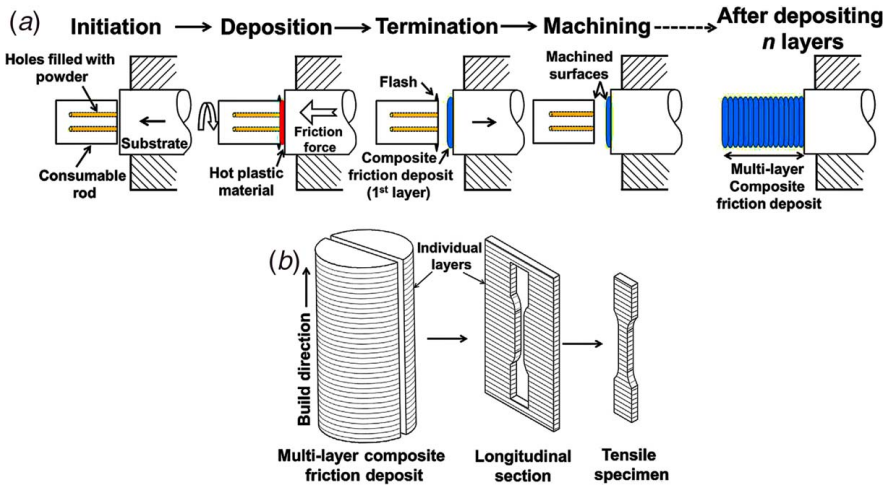

Fig. 12 (*a*) Schematic of the composite friction deposition process and (*b*) illustration of how flat tensile test specimens were extracted from cylindrical multilayer composite friction deposits [49] (Reprinted with permission from Elsevier © 2016)

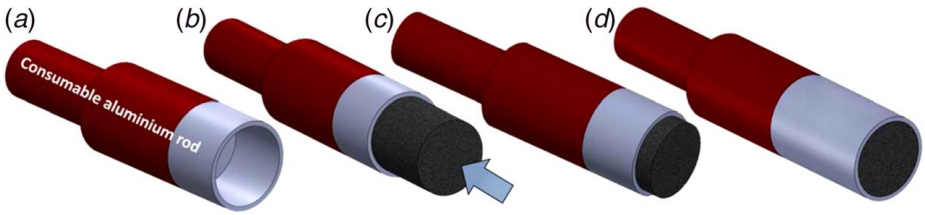

Fig. 13 Schematic representation of tool assembly for powder metallurgy-assisted friction surfacing [52] (Reprinted with permission from IOP Publishing, Ltd. © 2012)

with strong bonds between layers and uniform distribution of Ti particles, as was reported by Karthik et al. [49]. Also, friction surfacing of the Ti-6Al-4V composite reinforced with TiC particles onto the surface of Ti-6Al-4V substrate was studied by Belei et al. [123]. Holes were drilled at the tool tip and filled with TiC particles. It was found that hole placement on the tool influenced the efficiency of deposition, process behavior, coating quality, and particle distribution in the coating layer.

The fabrication and the characterization of composites made of aluminum–graphene were studied by Sharma et al. [54]. The impregnation process of graphene nano platelets into an aluminum alloy substrate using the modified friction surfacing technique employing a tool fabricated via powder metallurgy approach was accomplished by coating an aluminum–graphene composite rod, created by powder metallurgy, onto an aluminum substrate. Esther et al. [53] studied sliding wear behavior in friction surfacing of AA2124/4wt %B_4C nano-composite onto the Ti-6Al-4V substrate using the pin-on-disc technique. The consumable material was provided by the stir casting approach. The wear test result shows that the wear-rate of the deposition was smaller than that of the substrate due to the smaller friction coefficient. The electron backscatter diffraction (EBSD) analysis exhibited that the coarse grain structure in the nano-composite consumable tool was converted to ultra-fine grains from dynamic recrystallization. Mohanasundaram et al. investigated the friction surfacing of AA6061-B_4C composite consumable rod onto AA6061 substrate to find the optimum percentage of the B_4C particles [50]. Different consumable rods were prepared with various particles B_4C weight percentages of 0, 3, 6, 9, and 12 employing the stir casting machine. The reinforcement boron carbide particles were added into the molten AA6061 and stirred.

In a recent investigation, Özler et al. [51] studied the wear resistance and microhardness of coating of AA7075 consumable rod onto the AA5754 substrate using two different approaches, entitled friction surfacing with powder laying and powder sintering. In the powder laying approach, the boron carbide (B_4C) powder was laid on the surface of the substrate and then subjected to friction surfacing. In the powder sintering approach, a powder mixture including B_4C and aluminum was prepared and inserted into the consumable rod with an inner diameter of 15 mm and an outer diameter of 20 mm, and then it was sintered. A homogeneous deposit was not possible with the powder laying approach; however, a uniform deposition structure was possible using both powder-free depositions and multilayer gradient depositions in the sintering approach.

Sharma et al. [52] studied the powder metallurgy technique in surface modification of aluminum alloys through the friction surfacing process. The customized consumable rod containing graphite reinforcement utilized for surface modification was provided through a conventional powder metallurgy route, as presented in Fig. 13. The results of the experiments revealed a decreased wear-rate in the aluminum deposition reinforced by graphite due to the interlayer sliding attribute of the graphene layers. Moreover, adding graphite provides a reduced localized adhesion in the surface of the deposition, which results in a lower local adhesion and surface delamination.

2.3 Refill Friction Stir Spot Welding. Pandya and Menghani [59] studied a new approach for filling the keyhole left by friction stir welding (FSW) in lap joints. Tools were made of nonconsumable steel shoulder, and consumable aluminum joining pins of various geometries coupled with several pin insertion methods were used to fill the exit hole. Mechanical properties and microstructures of the resulting joints revealed a 7% increase of strength as compared to joints with the nonfilled exit hole. Zhang et al. used a T-shaped filler bit on the pin to fill the keyhole left by friction stir welding in 1060 aluminum, as shown in Fig. 14 [126]. In comparison with a cylindrical filler bit, the experimental result reveals improvement in the keyhole filling quality by greater fracture load, and a fracture location far from the interface, although small gaps were present at the bottom and lower periphery interface.

Huang et al. studied the filling friction spot welding (FFSW) technique using a consumable tool bit to fill the keyhole [55]. The semi-consumable joining tool with nonconsumable steel shoulder and consumable aluminum alloy joining bit (sizes for comparison) was created to produce a joint on an Al–Cu–Mg aluminum alloy sheet. Huang et al. [56] and Han et al. [57] studied the FFSW of rolled AA2219 plates with a semi-consumable tool equipped with a nonconsumable alloy steel shoulder, and consumable AA7075 and AA2219 bits, respectively. The result exhibits that the hardness is highest toward the center of the weld similar to the hardness profile measured in FSW.

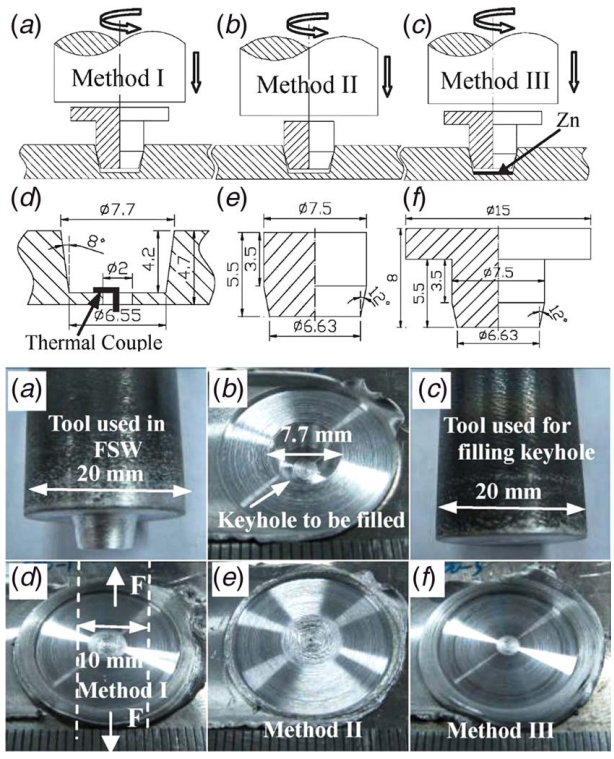

Fig. 14 Top: Illustration of the keyhole filling process using filler bits, (*a*)–(*c*) filling process, (*d*) keyhole, (*e*, *f*) filler bit. Bottom: Before and after keyhole filling process and used tools [126] (Reprinted with permission from Taylor & Francis © 2014).

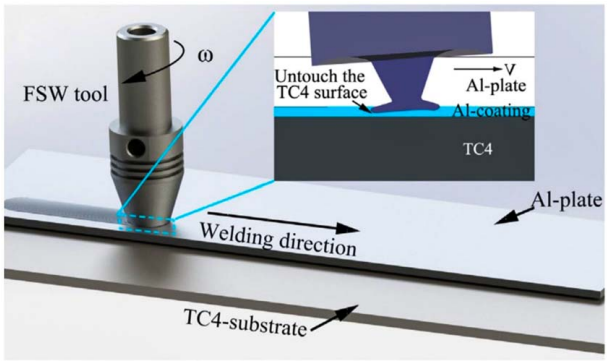

Fig. 15 The lap welding friction stir technique studied in Ref. [118] (Reprinted with permission from Elsevier © 2017)

Miles et al. presented an investigation on the friction surfacing process of a consumable joining bit on 980 dual-phase (DP) steel and a combination of 980 dual-phase steel and AA5754-O [80] to solve the problem of brittle intermetallic formation in fusion welding method such as resistance spot welding. Miles et al. [81] made a spot joint between 5754 aluminum alloy and a high-strength steel plates with a consumable joining bit. This investigation focused on joints composed of DP 590 and DP 980 steel bonded to AA5754-O using friction bit joining. It was revealed that the design of the joining bit employed in this method has a significant influence on the joint strengths.

Huang et al. studied a new hybrid method of FSW assisted by the friction surfacing technique for joining aluminum and titanium alloys, as shown in Fig. 15 [118]. In this method, a consumable rod with a concave surface on the end of the tool with an enlarged head was made to increase the material flow and the lap width. Shen et al. experimented the refill friction stir spot welding method in a 0.8 mm thick 7075-T6 aluminum alloy with varying process parameters such as welding time and axial plunge depth [58].

2.4 Additive Friction Stir Deposition by Using Friction Surfacing. Friction-based additive manufacturing is the application of solid-state friction stir technique for fast and scalable additive manufacturing of a wide range of metallic materials and matrix composite [138]. Friction-based additive manufacturing can be accomplished by different techniques such as rotary friction welding, friction deposition, friction surfacing, linear friction welding, friction stir additive manufacturing, and additive friction stir deposition (AFSD), as presented in Fig. 16 [137].

This review focuses on the deposition of material by a consumable tool; therefore, only AFSD, commercially known as MELD [144], was included in this review. AFSD was recently developed with a feed material in the form of either a solid-rod or a powder delivered to the deposition zone through a nonconsumable rotating hollow shoulder under hydrostatic pressure, as presented in Fig. 17. Frictional heat is developed at the interface of the rotating feed material and substrate, which leads to solid-state thermal softening of the feed material. The consumable material undergoes large plastic deformation and shear strain rate as it is forced through the rotating tool onto the substrate [146,147]. MELD can be

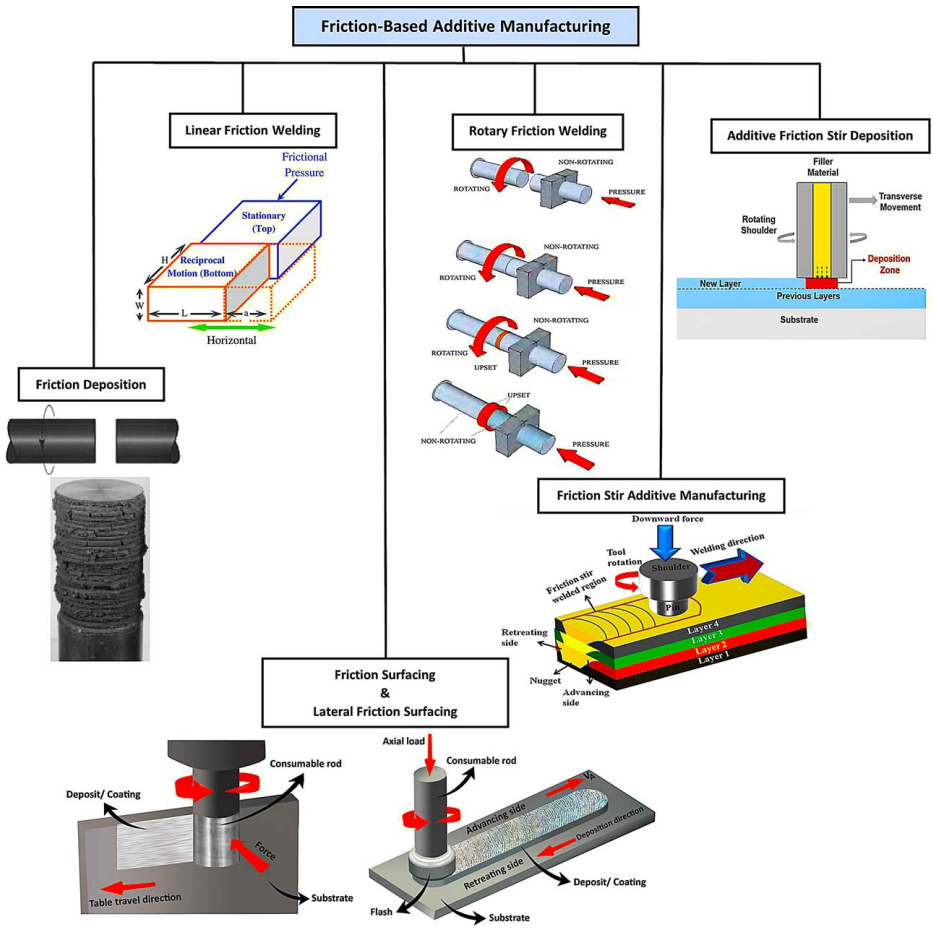

Fig. 16 Classification of existing friction-based additive manufacturing techniques [15,139–143] (Reprinted with permission from Elsevier © 2012; Creative Commons Attribution 3.0 Unported (CC BY 3.0); Elsevier © 2015; Elsevier © 2018)

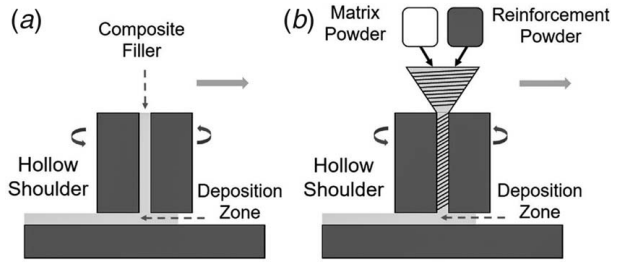

Fig. 17 MELD process by employing (*a*) a solid composite rod and (*b*) matrix and reinforcement powders as the feed material [145] (Reprinted with permission from Springer Nature © 2018)

applied for additive manufacturing, metal joining, solid-state coating applications, surface modification, and repair [144].

As the tool moves across the workpiece, a single track of material is deposited onto the substrate. Once the first layer is deposited, the height of the tool increases to start the second layer as in additive manufacturing. Multiple deposit layers can be created by forging the feed materials onto the surface of the previous layer, as shown in Fig. 18. There is no melting or rapid solidification, enabling strong metallurgical bonding with minimal porosity, hot cracking, distortion, and residual stresses [143,147]. Several important process parameters, such as axial forging pressure, tool rotational speed, and traverse speed, influence the thickness and the quality of the deposited material [138].

The novel friction-based additive manufacturing technique, additive friction stir deposition, is studied for depositing different materials such as aluminum [148–152], Inconel [153,154], magnesium [155], titanium [156], and copper [151,157]. Tools made of tool steel are suitable for depositing low-strength materials; however, a tool made of high-toughness materials such as polycrystalline cubic boron nitride or tungsten carbide should be employed for depositing high-strength materials [145]. Higher reinforcement loading results in a higher level of wear and degradation in the tool, which may limit AFSD for fabricating very hard composites; however, this is not an issue in the friction surfacing technique.

Due to the severe material deformation and flow, the AFSD technique has a high level of flexibility with the feed material quality, even if the consumable material is not fully dense or contains oxides [158]. The AFSD technique is ideally appropriate to process a metal waste to create a solid-state deposit. This concept presents the potential to recycle metal machine chips as the feed material in the AFSD process. Jordon et al. employed this approach to feed AA5083 chips with 2–3 mm in length directly into the AFSD process, as presented in Fig. 19 [159]. This process resulted in a deposit with 6 mm in height, with fine grain structure resulting from dynamic recrystallization and mechanical properties similar to the wrought material.

Fig. 18 Multilayer deposit of AA2219 developed by the AFSD technique [147] (Reprinted with permission from Elsevier © 2021)

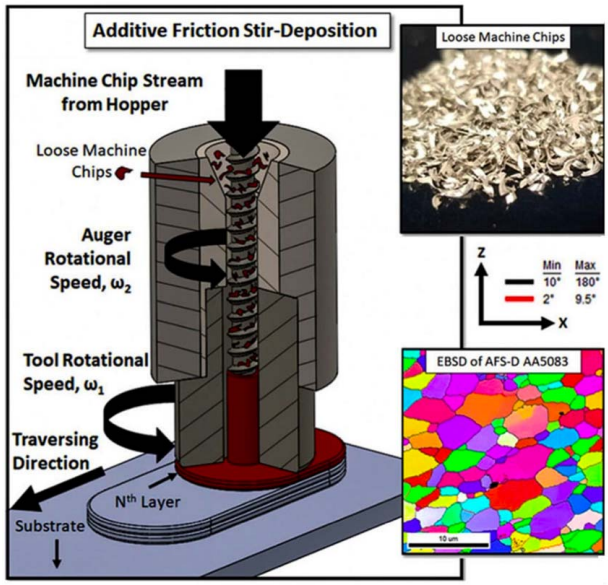

Fig. 19 Illustration of the recycling technique using AFSD [159] (Creative Commons Attribution 4.0 International (CC BY 4.0))

3 Characterization of Thermomechanical Transfer and Structure of Deposition

In this section, the relationship between process parameters and material transfer is analyzed. Friction surfacing is a process with a high level of complexity that depends on various parameters. The process factors involved in this technique directly influence the deposit quality. In this process, the machine parameters include all process factors related to the machine, such as tool rotational speed, axial load, and traverse speed. The environment parameters are the factors related to the environment in which the deposition occurs, such as the temperature of the environment, shielding gas type, and its flowrate. The most important consumable tool parameters are dimensions and material of the consumable rod and substrate. The process parameters are controlling variables affecting process temperature and coating properties such as geometry, surface roughness, hardness, microstructures, bonding quality, wear and corrosion performance, and residual stress. Investigation of the effects of process factors was discussed by Sugandhi and Ravishankar [65]. Achieving an appropriate energy input using suitable process parameters during friction surfacing may enable control of flash formation. Advances in analytical mathematical analysis of the process are needed to facilitate optimization of experimental tests, as is considered by Vitanov and Voutchkov [93].

The minimization of wasted material (flash) is another critical issue that has been studied. Gandra et al. exhibited that in some experimental tests, flash-based material lost of approximately 40–60% of the total tool consumption [21]. Vilaça et al. showed that in the friction surfacing approach, the primary flash occurs around the consumable tool and grows in the tool axial direction toward the clamping zone [19]. If the primary flash growth is constrained in the axial direction, then secondary flash starts and grows parallel to the surface of the substrate. Since the secondary flash stays in contact with the surface of the deposition, it may influence the process. The formation of the secondary flash has a beneficial effect on the hardness of the deposited material and the efficiency of the process. This is an important point that represents several opportunities for industrial applications and a new area of study for further research to improve the friction surfacing process.

3.1 Deposition Width and Thickness. Most of the parametric studies focus on the resulting coating width and thickness. At this early stage in friction surfacing research, the most important

qualities of the coating remain to be improved and controlled. Galvis et al. investigated the effects of process factors on the deposition of AA6351-T6 over AA5052-H32 in a conventional mill [28]. The feed rate was employed as a control factor, and the microstructural and superficial characterization of the deposition layer was studied. It was exhibited that a conventional machine is capable to produce deposited layers of a homogeneous material with deposition rates increasing with the increasing travel speed.

Sahoo and Mohanty experimentally studied different combinations of process factors in friction surfacing 6063 aluminum alloy onto EN24 carbon steel using different rod diameters, 12, 18, and 24 mm [66]. A decrement in the thickness of the material deposition with an increment of the axial force and the tool rotational speed was observed. Also, higher tool rotational speeds resulted in a wider coating layer. Generally, the deposition width was dependent on the diameter of the tool, which was typically in the range of 0.9–1.2 times the rod diameter, as shown by Vitanov and Voutchkov [93].

AA6063 aluminum alloy was coated on AISI 316 stainless steel by Sahoo et al. with three different tool diameters of 14, 18, and 22 mm [67]. It was found that the increasing axial load and decreasing tool rotational speed resulted in the increasing deposition width. Higher tool rotational speed resulted in lower deposition thickness values. In a recent investigation by Sahoo et al. [68], aluminum 6063 was friction surfaced on the preheated EN8 medium carbon steel substrate at 100 °C, 200 °C, and 300 °C using a custom-made vertical milling machine. Applying higher tool rotational speed at a constant forging force developed thinner coating layers. It was also revealed that increasing the substrate temperature results in a thick viscoplastic material transformation and fewer pores and cavities at the interface.

Gandra et al. investigated the friction deposition of AA6082-T6 onto the surface of AA2024-T3 substrate [29]. It was found that low travel and rotational velocity resulted in increased coating thickness and width. Figure 20 presents the influence of travel speed on the deposition thickness, width, and bonded width. Elevated travel speeds resulted in thinner deposition layers since the travel speed affected the rate at which the rod material was transferred to the substrate.

As shown in Fig. 21(*a*), the increased axial force resulted in a wider and thinner coating and thus improved the bonding width. The tool rotational speed affected the deposition width and the bonding quality (Fig. 21(*b*)). Although it is experienced that lower to intermediate tool rotation speeds improve the quality bending, higher tool rotation speeds provided a more flat and regular coating.

A study was carried out by Kumar et al. to investigate the relationships between process parameters and geometry of 6063 aluminum alloy friction surfaced deposition onto IS2062 substrate [69]. Physical parameters such as axially applied force, tool rotational speed, and table travel speed were reported to have the most influence on physical dimensions. Deposition thickness decreased as the deposition width increased. More recently, Vasanth et al. investigated friction surfacing of A6063 aluminum alloy consumable rod onto the mild steel IS-2062 E250 CU [70]. Seventeen different experiments using different values for critical process parameters such as tool rotational speed, traverse speed, and axial load were carried out. The thickness of the depositions was recorded between 1.11 and 2.67 mm, but only coatings with thickness values between 1.78 and 2.00 mm exhibited good corrosion resistance in acidic and salt solutions.

Nixon et al. investigated friction surfacing deposition of AISI 316 stainless steel alloy onto the surface of EN24 carbon steel substrate [94]. The traverse speed, tool rotational speed, and axial force were remarked as the most effective factors. They exhibited that the depth of the deposition layer decreased as the deposited coating width increased. Sahoo et al. studied the effects of substrate preheating on the geometry of the coatings [95] and optimum process parameters [96] during the friction surfacing of AISI 316 stainless steel onto the EN24 medium carbon steel substrate. The inductive preheating of the substrate was done with an electric unit with three

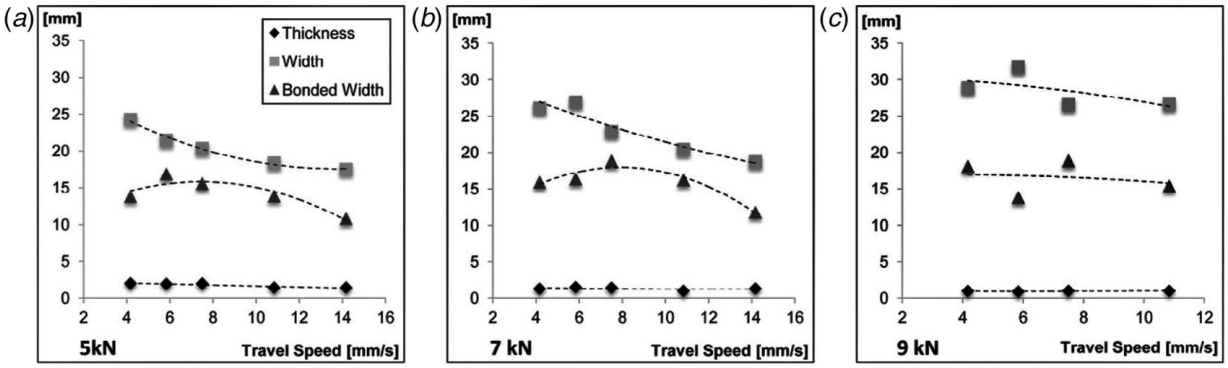

Fig. 20 Effect of the travel speed on coating thickness, width, and bonded width for (*a*) 5 kN, (*b*) 7 kN, and (*c*) 9 kN axial forces and a 3000 rpm rotational speed [29] (Creative Commons CC-BY-NC-ND license)

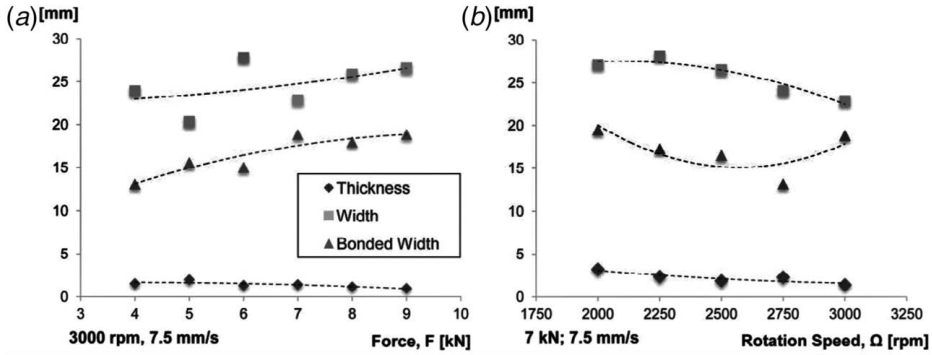

Fig. 21 Effect of force and rotation speed on coating thickness, width, and bonded width [29] (Creative Commons CC-BY-NC-ND license)

different temperatures of 200 °C, 400 °C, and 600 °C, and the deposition rate and material consumption rate were measured. It was noticed that increasing the tool rotational speed resulted in a wider but thinner deposit.

Rafi et al. studied friction surfacing deposition of H13 tool steel onto the substrate of low carbon steel [97]. The substrate travel speed did not significantly affect the deposition width. For all substrate travel velocities, the width of the deposited coating was bigger than the diameter of the consumable rod (18 mm). On the other hand, increasing the tool rotational speed resulted in a significant reduction in the deposition width. This phenomenon was explained by the concept of "real rotational contact plane," which refers to the actual/instantaneous contact plane between the substrate surface and the consumable tool in the process. The area of the real rotational contact plane is reduced with the increased tool rotational speed.

Kumar et al. identified suitable process factors for friction surfacing [71]. Their analysis exhibited that higher axial pressing force resulted in lower deposition thickness and higher bend ductility. Recently, fuzzy logic was used to predict the width and thickness of the coatings by Murugan et al. [128]. In the friction surfacing process of these materials, it was observed that increasing the axial pressing force increased deposition width and thickness.

Friction surfacing of 6063 aluminum alloy onto AISI316 stainless steel and the relation between the process variables and deposition dimensions was studied by Sahoo et al. [72]. In this study, the effects of process parameters such as axial force (4, 5, 6 kN), tool rotational speed (2000, 2400, 2800 rpm), and table travel speed (75, 150, 225 mm/min) on deposition width and thickness were studied. It was observed that increasing the axial load and decreasing the tool rotational speed increased the deposition width. The coating thickness decreased when the tool rotational speed and axial force increased. Guo et al. successfully fabricated the stainless steel 316L coatings onto 304 substrates [18]. Figure 22(*a*) shows a transverse cross-sectional view of deposition at 1500 rpm. Increased spindle speed caused a decrease in both the width and thickness of the deposition, as shown in Fig. 22(*b*).

The influence of process parameters on the coating geometry discussed in this section is summarized in Table 3. The major conclusion is that no clear trend can be established. Intuitively, it makes sense that the increased force would result in wider deposition, which is presented in Table 3 especially for the aluminum tool, and increased travel speed would result in decreased width and thickness. In general, there seems to be a proportional relationship with parameters and width, and an inverse relationship between parameters and thickness. There is more of an inverse relationship between spindle speed and dimensions.

3.2 Effect of Process Parameters on Temperature. The effects of parameters on heat generation and temperature during the process have also been studied. Some of these include modeling studies, as spatial temperature profiles are difficult to measure. Different combinations of process parameters in friction deposition of A6063 aluminum alloy onto EN24 carbon steel were experimentally studied by Sahoo and Mohanty [66]. In this investigation, three different rod diameters of 12, 18, and 24 mm were employed. The process temperature profile was measured with a noncontact infrared thermometer, and the successful depositions were subjected to Vickers microhardness and bending tests. In addition, energy-dispersive X-ray analysis and field emission scanning electron microscopy techniques were utilized to evaluate microstructure and intermetallic bonding features. The temperature–time graph demonstrated in Fig. 23 presents the thermal profile of friction surfacing using different rod diameters from the start of tool rotation to the end of the process. The 24 mm tool diameter provided the highest peak temperature; however, the temperature distribution at the interface was not uniform and steady.

Silva et al. [98] investigated the friction surfacing of AISI 4340 alloy steel onto ASTM A36 low carbon steel substrates with varying process factors, while the process temperature evolution was monitored by means of an IR camera. In this study, several experimental tests were carried out to investigate the influence of the initial substrate surface roughness and the process parameters. Due to the flash formation, the highest value of deposition efficiency was recorded as 60%. The result of the experiment revealed that the substrate surface roughness had no significant influence on the process temperature. Also, the high cooling rate associated to the friction surfacing process resulted in the formation of martensite in the deposit.

Friction surfacing of A5083-H112 consumable tool onto A7050-T7451 substrate and the associated critical process parameters and process temperature were investigated by Kallien et al. [30]. The process temperature measurement was carried out from K-type thermocouples inserted in eight holes drilled on the backside of the substrate up to 0.5 mm below the surface of the substrate. A set of process parameters including the tool rotational speed of 1200 rpm, traverse speed of 6 mm/s, and axial force of 8 kN was employed as the reference process parameters, which resulted in the maximum process temperature of 394.8 °C. It was found that increasing the tool rotational speed to the values more than the reference point hardly affects the maximum process temperatures. Also, decreasing the traverse speed by 2 mm/s increased the maximum temperature by approximately 50 °C; however, no noticeable influence on the maximum temperature was observed by increasing the traverse speed by 2 mm/s. It was noted that increasing the process temperature results in wider and thinner deposits.

Residual stress is an important factor that should be investigated in friction surfaced deposit and substrate. Residual stress exists within a body even when no external force is applied. It may be added to, or subtracted from, all applied stresses on a part. The residual stress may result in an unexpected failure if it is combined critically with all other applied stresses. Therefore, it is essential to understand the origins of residual stress during the process to decrease the chance of developing harmful residual stresses. Residual stresses arise due to incompatibilities between different zones of the material in a body. Plastic deformation, localized heat treatments, composites, and multiphase materials can develop residual stress within the body [160]. Finite element method (FEM) is a thermomechanical simulating approach that can be employed to investigate the residual stress distribution. Recently, several attempts have been made to simulate the friction surfacing process using a finite element model.

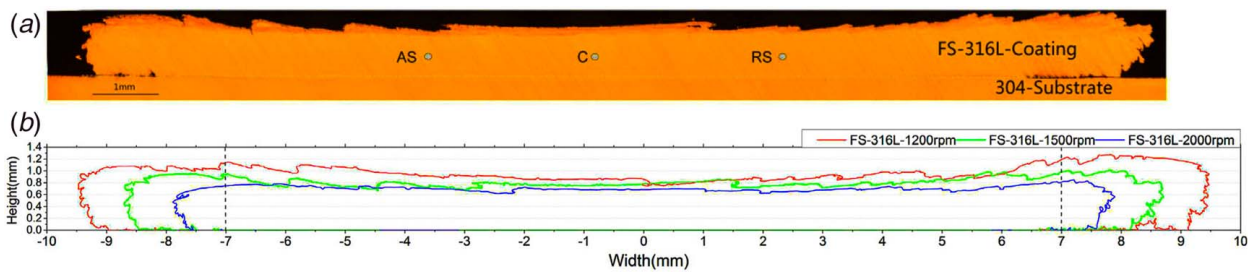

Fig. 22 (*a*) Coating cross section produced at 1500 rpm by optical microscopy and (*b*) friction depositions using the different tool rotational speed (dash lines show the tool diameter) [18] (Reprinted with permission from Elsevier © 2019)

Table 3 The influence of process parameters on the coating geometry

Ref.	Tool material	Substrate material	Influence of process parameters on the coating width and thickness
[93]	AA6351	AA5052	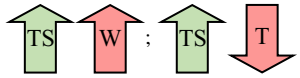
[28]	AA6063	EN24	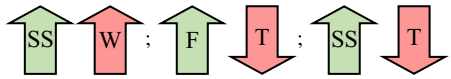
[66]	AA6063	AISI 316	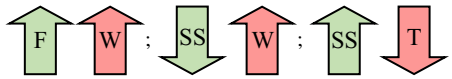
[67]	AA6063	EN8	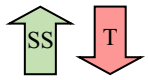
[68]	AA6082	AA2024	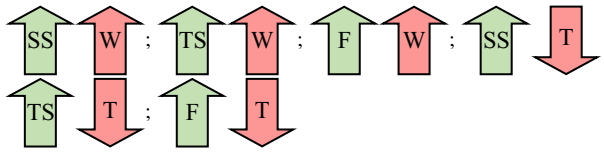
[29]	AA6063	IS2062	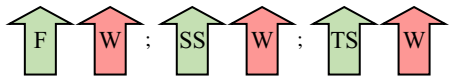
[69]	AA6063	IS-2062-E250Cu	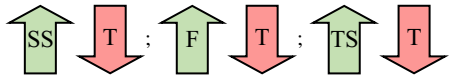
[70]	AISI316	EN24	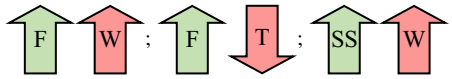
[94]	AISI316	EN8	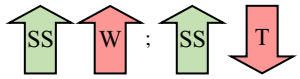
[95]	AISI316	EN8	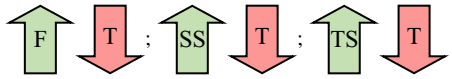
[96]	H13	Low Carbon Steel	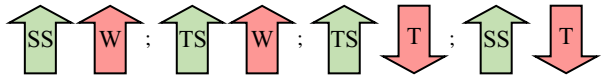
[97]	AA6063	Mild Steel	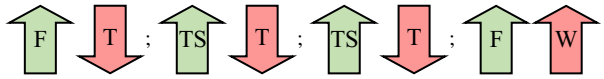
[71]	Monel 500	AISI 1012	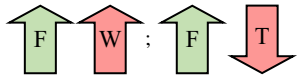
[128]	AA6063	AISI316	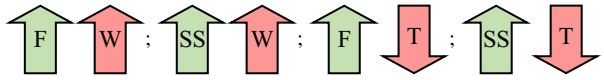
[18]	AISI 316L	AISI 304	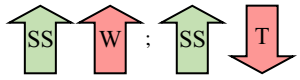

Pirhayati and Aval developed a three-dimensional finite element model to simulate the thermomechanical behavior of the friction surfacing process of AA2024 consumable rod onto a 2 mm thickness AA2024 sheet [31]. The model output of maximum temperatures on the advancing and retreating side was very similar due to the high thermal conductivity of the deposited material. Plastic strain values at the center of the consumable tool tip were greater than those at the edges. Moreover, the simulation predicted a weaker bonding strength between the deposition and substrate on the advancing side, which is due to a higher strain rate on the advancing side. The very high cooling rate at the interface of the coating and substrate resulted

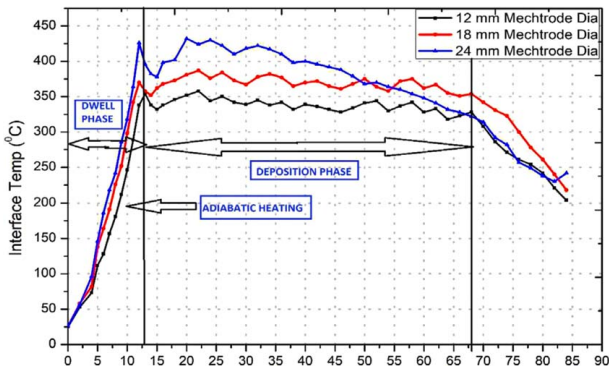

Fig. 23 Thermal profile obtained from the IR thermometer for different consumable rod diameters [66] (Creative Commons Attribution 4.0 CC BY 4.0)

in three times finer grain size compared to the top surface of the deposition.

Bararpour et al. studied friction surfacing of AA5083 consumable rod onto the AA5052 substrate [32]. In this study, ABAQUS finite element modeling software was utilized to anticipate the thermomechanical behavior of materials in this process. The model revealed that the maximum values of temperature and strain rate occurred at the upper surface of the deposition in the advancing side; however, the maximum temperature in its advancing side and retreating side was not very different owing to the high thermal conductivity of aluminum. Bararpour et al. developed a coupled thermomechanical simulation and experimental analysis to study the influence of process parameters of the friction surfacing process on the residual stress distribution and the flow field [33]. In this study, the aluminum alloys AA5083 and AA5052 were the consumable tool and substrate materials, respectively. It was observed that higher heat input caused higher material flow, and subsequently, a larger velocity vector. Moreover, increasing the translational speed at a constant tool rotational speed and a feeding rate decreased the extent of the tensile residual stress zone. Also, increasing the tool rotational speed at a constant feeding rate and translational speed decreased the maximum tensile residual stress and the extent of the tensile residual stress field.

The influence of the axial feeding rate on the deposited coating of AA2024 onto AA1050 aluminum alloy substrate was investigated by Rahmati et al. [34]. Several combinations of process parameters were examined, and the tool rotational speed of 1000 rpm and translational speed of 125 mm/min were selected as the optimum parameters to provide the maximum deposition efficiency. It was also observed that more flash was formed on the advancing side, while the axial feeding rate value was greater than translational speed. Also, Rahmati et al. developed a finite element model for friction surfacing of AA2024 onto a substrate of AA1050 [35]. ABAQUS was used to model the thermomechanical behavior of the material deposition during the process. The highest level of plastic strain occurred on the advancing side of the friction deposition. The lower temperature in friction surfacing and heat conduction through the substrate caused a decrease in both the material flow and plastic strain. Figure 24 shows that the maximum strain rate and temperature occurred at the end of the consumable rod in direct contact with the deposition.

4 Metallurgical, Chemical, and Mechanical Properties of the Deposition

4.1 Metallurgical Study. This technique produces metal deposition at temperatures less than the consumable material's melting point, followed by intense cooling rates, which make this technique a great alternative for creating a fine-grained coating with higher corrosion and wear resistance performance. In the multilayer friction surfacing deposition process, it is important to understand microstructural development in heat treatable aluminum

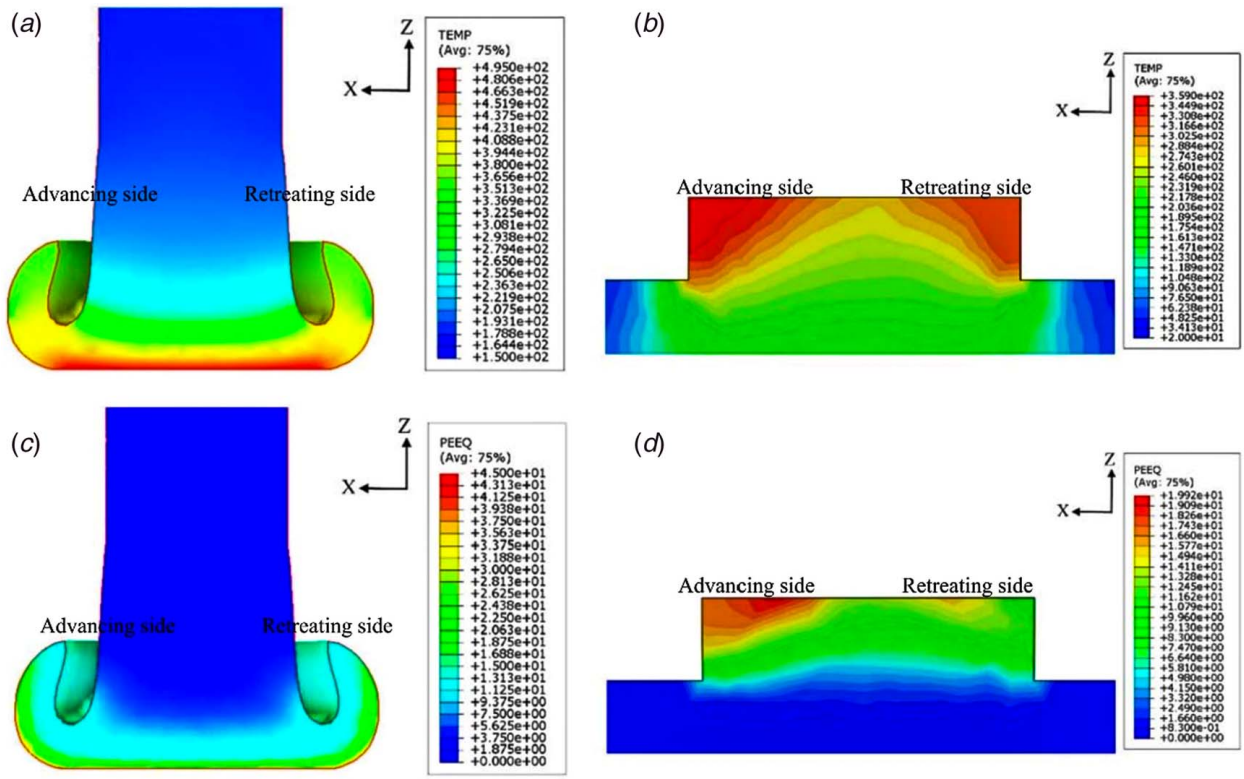

Fig. 24 Illustration of temperature and plastic strain rate distributions: (*a*) temperature in the tool, (*b*) temperature in the coating, (*c*) plastic strain rate in the tool, and (*d*) plastic strain in the coating [35] (Reprinted with permission from IOP Publishing, Ltd. © 2013)

alloys. This section highlights those studies focusing on structure/property characterization.

Several kinds of inspection techniques such as SEM, X-ray diffraction testing, optical microscopy, tensile testing, roughness testing, microstructural analysis, and hardness testing have been carried out to investigate the deposited coating quality. It was shown by Dilip and Ram that friction surfacing invariably causes overaging of the strengthening precipitates in various heat treatable materials [36]. For this problem, a solution posttreatment can be utilized; however, it may cause other issues such as abnormal grain growth. Suhuddin et al. examined the microstructural evolution in depositing material during friction surfacing of 6082-T6 aluminum alloy onto a substrate made of AA 2024-T351 by employing the electron backscatter diffraction method [37]. In this study, crystallographic data were achieved from several different areas in the deposited coating and consumable tool. It was exhibited by the textural analysis that material flow can be explained by simple-shear deformation and resulted in significant grain refinement. Furthermore, the electron backscatter diffraction has been employed to study the deposition of 6082-T6 aluminum alloy onto 2024-T351 aluminum alloy [37].

The deposition of 6351-T6 aluminum alloy onto the substrate of AA5052-H32 was investigated in Ref. [46]. In this study, holes were drilled in the consumable tool, which were filled with reinforcing Al_2O_3 particles. Postprocessing investigation of the consumable rod identified lower hardness values in region I (see Fig. 25), with respect to as-received condition hardness values. This is attributed to thermal conditioning of the rod resulting in a loss of the T6 heat treatment condition, and the microstructure of the rod in this region was like the as-received material. With region II being closer to the friction surface the hardness was HV60-65 and exhibited a coarse grain structure. Thus, regions I and II are clearly heat-affected zones. Region III exhibited both thermal and mechanical processing where the mechanical loading included both compressive and torsional loading. For example, a set of grains were deformed in the direction of the flash layer formation, refer to Fig. 25(*d*), with greater mechanical deformation allowing for recrystallization to occur, refer to Figs. 25(*e*) and 25(*f*).

It was shown by Fitseva et al. that the deposition of Ti-6Al-4V onto Ti-6Al-4V substrate under high rates of deformation resulted in microstructural grain refinement and a corresponding improvement of mechanical properties in the deposited coating [119]. The tool material consumption rate was found to be an efficient controlling factor for deposition. Tool rotational speeds of 400, 600, 3000, and 6000 rpm and deposition speed of 16 mm/s were used, and all these parameter sets resulted in the creation of coatings without flash. The result of this study also shows that smoother coating surfaces were obtained using the lower tool rotational speeds, and higher tool rotational speeds resulted in rougher coating surfaces. Flash formation can be controlled with low energy input using the appropriate deposition rate and the tool rotational speed. Vale et al. friction surfaced titanium (Ti) grade 1 and Ti-6Al-4V onto Ti-6Al-4V hot-rolled plates to analyze the material processing behavior and the deposition properties [120]. A constant tool consumption rate was employed during the process, and it was found the axial loads were about ten times higher in the friction surfacing of Ti-6Al-4V than Ti grade 1, which is due to the higher strength of Ti-6Al-4V. The analysis revealed a higher peak temperature for Ti grade 1 compared to Ti-6Al-4V.

Monolayer friction surfacing of magnesium alloy AZ91 casting tool onto magnesium alloy AZ31 substrate was studied by Nakama et al. [132]. Also, monolayer and multilayer friction surfacing of aluminum alloy A2017 rod on aluminum alloy 5052 substrate plate was investigated by Tokisue et al. and the effects of process factors on microstructures and mechanical properties of both monolayer and multilayer deposition were explored [38]. In both monolayer and multilayer coatings, microstructures exhibited improved properties compared to those of the consumable rod

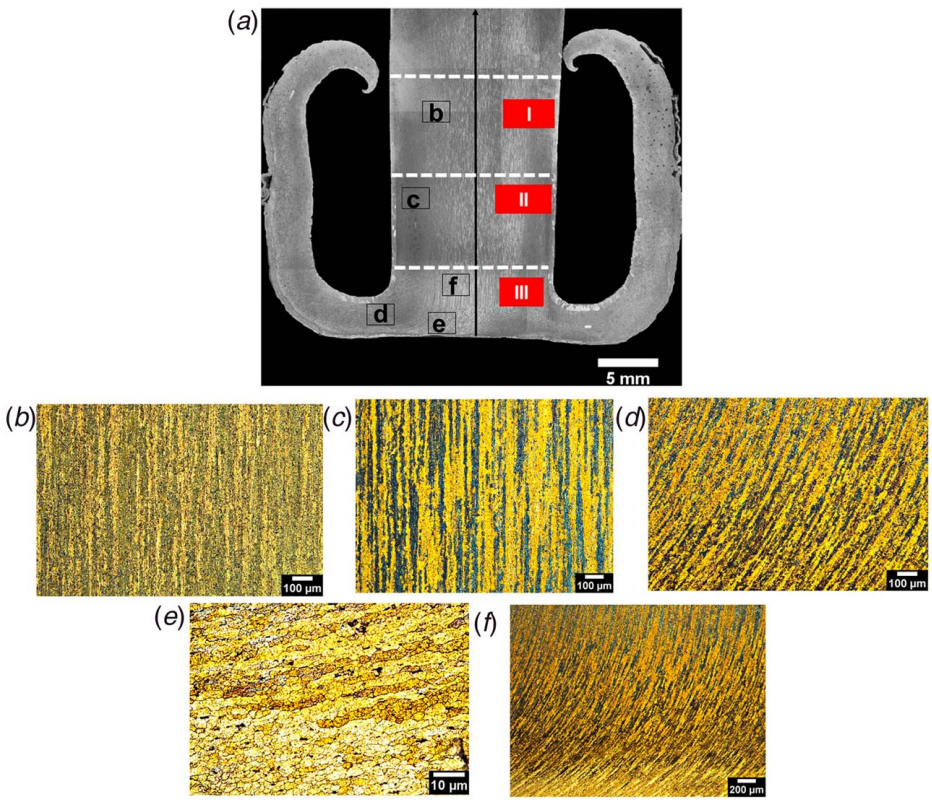

Fig. 25 (*a*) Microstructural evolution of consumable rod, (*b*) consumable rod T6 condition microstructure, (c) microstructure of coarse grains in the HAZ, (*d*) grains aligned in the strain direction at the rod tip, and (e) and (*f*) recrystallized grains aligned in the strain direction at the rod tip [46] (Creative Commons Attribution CC BY 4.0)

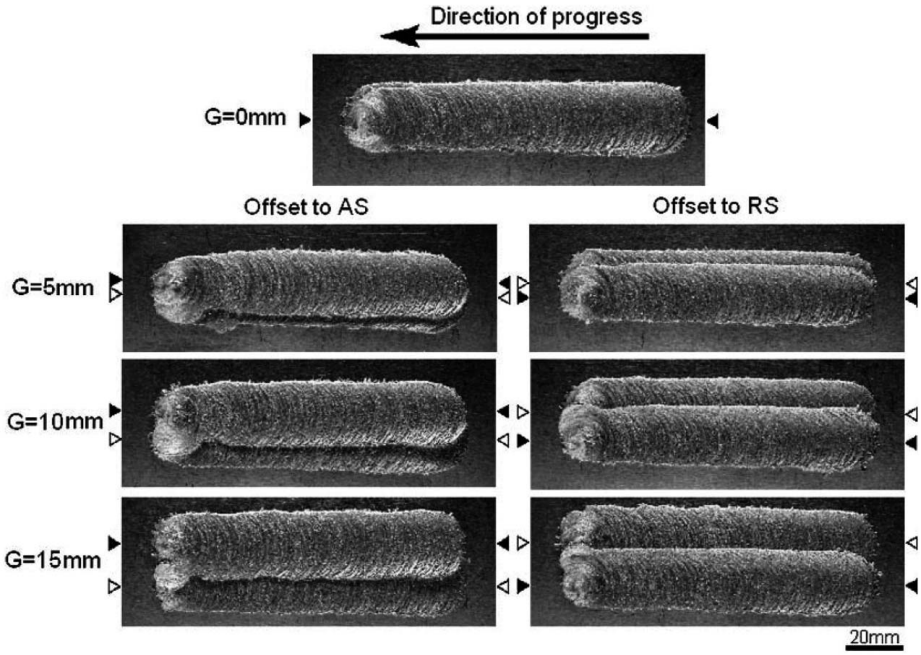

Fig. 26 Multilayer deposited layers, spindle speed 20.0 rev/s, traverse speed 9 mm/s, and friction pressure 30 MPa. Δ, first consumable rod's center; ▲, second consumable rod's center [38].

and substrate as recieved. It was exhibited that the monolayer deposition layer inclined toward the retreating side (right side) and that the second deposition layer of multilayer deposition approached the first deposition layer, as shown in Fig. 26. In another investigation [23], the single and multilayer deposits and butt joint through the friction surfacing technique using Al–5Mg aluminum alloy for both tool and substrate material were investigated. The average grain size in the coating layers was smaller than those in the substrate. Also, in the multilayer deposition, the minimum grain size was observed in the upper deposited layers due to the repeated heating of the lower deposit layers when the upper deposit layers are coated. The surface hardness in the deposition increased as the distance from the substrate interface increased.

In another investigation, Sekharbabu et al. employed the friction surfacing technique to create a defect-free deposited layer from D2 tool steel as the consumable material on the surface of a substrate made of low carbon steel [99]. Then, X-ray diffraction, optical microscopy, and SEM were employed to characterize the microstructure. The thermal profile was measured by the infrared thermography and the peak temperature was determined to be approximately 1200 °C. The SEM analysis highlighted that the carbides present in the deposition are finer in comparison to the as-received D2 tool steel, as presented in Fig. 27. This is the result of fragmentation of the carbides during the severe deformation in the friction surfacing process.

Guo et al. friction surfaced AISI 316L consumable rod onto the AISI 304 substrate using argon as a shielding gas for avoiding oxidation [100]. By increasing forced convection using argon shielding, it was observed that the average grain diameter increased in both surface and cross-sectional views of the deposition. However, this increment was more significant in the surface of the deposition in comparison to the cross section, because the crystal structure of the deposition in the cross section was dominated by the greater stress in the vertical direction. Also, Guo et al. found that the tool rotational speed employed in friction surfacing of stainless steel 316L onto 304 substrates had a more significant influence on the microstructure of the deposition surface than that of the cross section [18]. The DRX analysis showed that the hardness of the deposition improved compared to the as-received stainless steel 316L consumable tool. Govardhan et al. evaluated different factors and process parameters associated with the friction surfacing process to produce high-quality coatings and joints [101]. The metallography of the sample coated surfaces showed dense and fine microstructures, and no cracks were found in the HAZ.

Puli and Ram exhibited that in friction surfacing by moderate Zener-Hollomon parameter conditions, the AISI 316L stainless steel undergoes discontinuous dynamic recrystallization [102]. The coating layer of AISI 316L exhibited a growth in the size of grains starting from the interface of deposition and substrate toward the deposition surface. This is due to a decreasing cooling rate from the interface to the deposition surface. Fitseva et al. attempted to evaluate the effects of tool rotational speed of the rod on the microstructure, mechanical properties, and grain size evolution of Ti-6Al-4V [121]. Dovzhenko et al. investigated the influence of traverse speed on the residual stress in 2 mm thick substrates made from Ti-6Al-4V using synchrotron diffraction [122]. In addition, the influence of the residual stress on fatigue cracking was studied. The experimental results exhibited that higher traverse speed created high values of peak residual stress. Also, the coating layer thickness influenced the residual stress propagation.

Puli and Ram carried out an investigation to study and evaluate the deposition coating of AISI 410 developed by two different depositing methods, including metal arc welding and friction surfacing technique [103]. The microstructures evaluation, corrosion, and wear resistance performance of the deposited coating layers were discussed in detail. The experimental result exhibits no dilution in the friction surfacing method as an advantage for the technique. Also, the coating of AISI 410 provided by the friction surfacing technique presented wear and corrosion resistance performance comparable to AISI 410 in the hardened and tempered situation. The result of energy-dispersive X-ray spectroscopy (EDS) spot analysis on friction deposition and metal arc welding is shown in Fig. 28. The friction surfacing deposition presents no dilution with uniform chromium levels across the deposition thickness (Fig. 28(*a*)). In contrast, the metal arc welding deposition shows significant dilution at points 3 mm away from the deposition–substrate interface (Fig. 28(*b*)). The friction surfacing coating showed a significant lower wear volume than manual metal arc welding coating and comparable with that of the heat-treated bulk material in pin-on-disk wear tests.

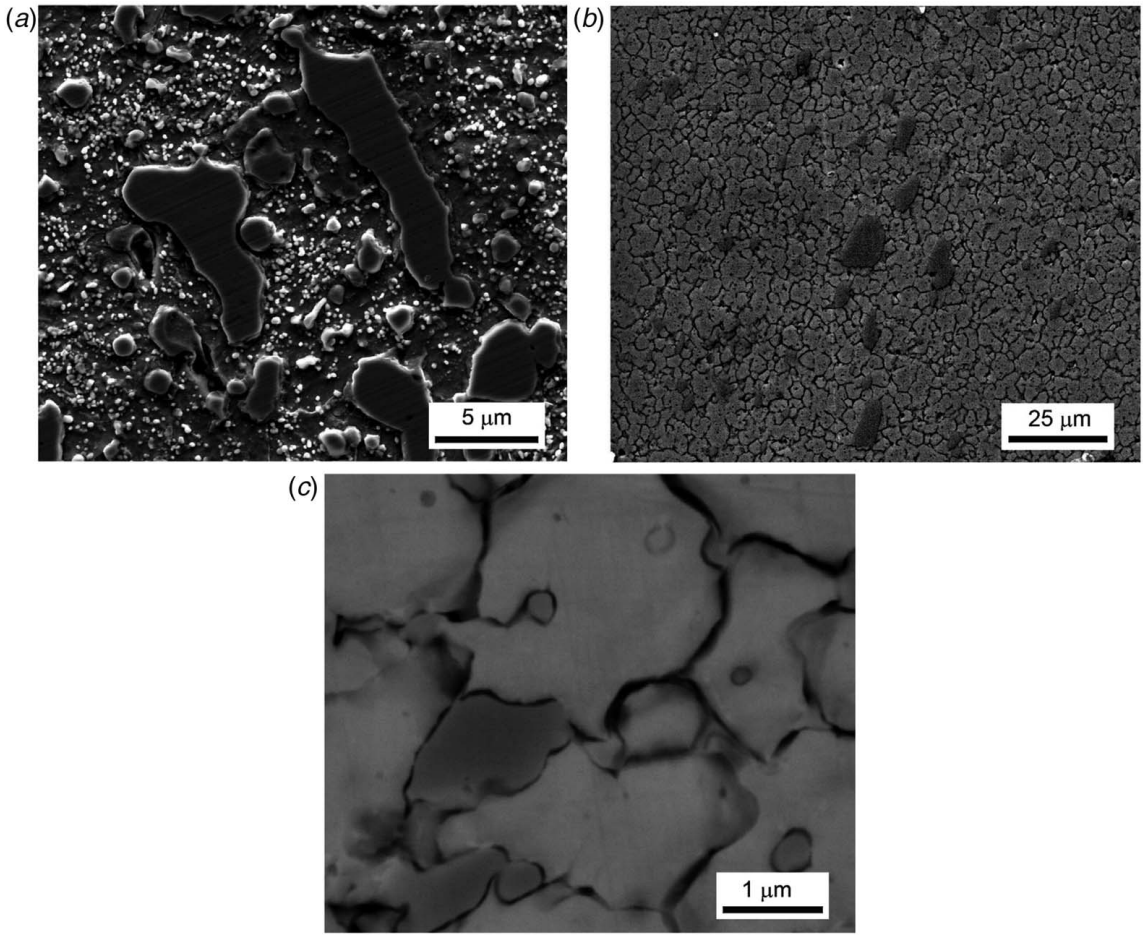

Fig. 27 D2 tool steel: (*a*) scanning electron microscope-secondary electrons (SEM-SE) image as-received consumable tool, (*b*) SEM-SE image deposit, and (*c*) scanning electron microscope-backscattered electrons (SEM-BSE) deposit [99] (Reprinted with permission from Elsevier © 2013)

Phillips et al. investigated the relationship between process parameters and microstructure, nanostructure, and mechanical properties [39]. In this study, aluminum alloy AA6061-T651 was selected as the material for both consumable rod and substrate. The result of EBSD analysis was significant grain size reduction from 200 μm in AA6061-T651 material as received to an average of 15 μm in the deposition. Moreover, the microstructure analysis revealed that a slower deposit resulted in a more recrystallized microstructure, which could have been a result of the decreased viscosity and strain near the edge of the consumable rod. Kumar and Bauri [116] and Kumar and Bauri [117] reported a new approach named reverse friction deposition, wherein the consumable rod utilized as a tool in the friction stir process curled up and created a deposition layer as a seamless tube over itself. The formed tube had improved oxidation behavior and a fine-grained structure. Yu et al. developed an ultra-fine-grained deposited coating of A6061 aluminum alloy onto the Q235 steel substrate [73]. This study shows that due to the continuous dynamic

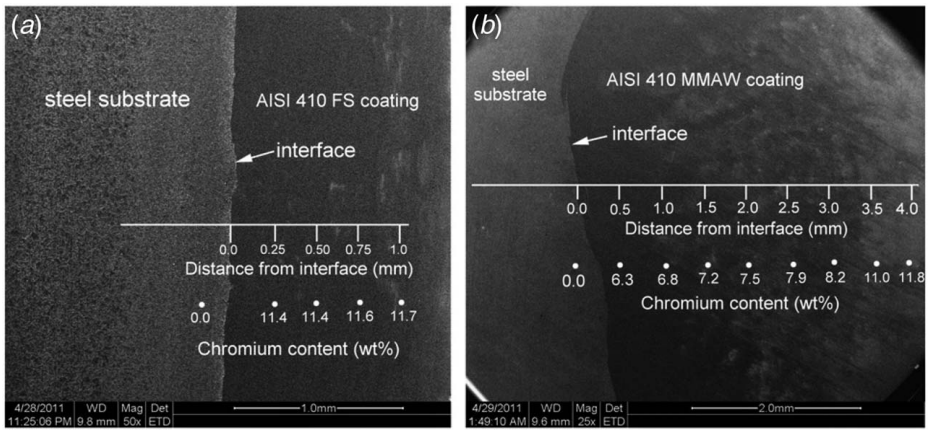

Fig. 28 Results of SEM-EDS spot analysis on (*a*) friction surfaced and (*b*) manual metal arc coatings [103] (Reprinted with permission from Elsevier © 2012)

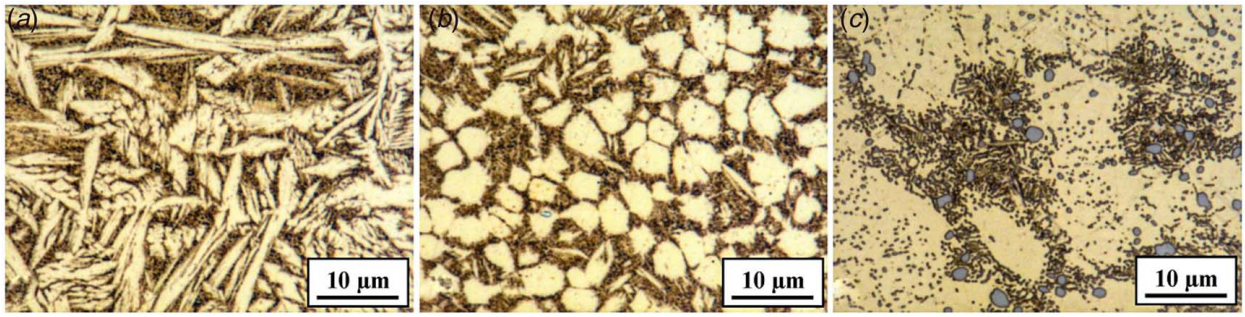

Fig. 29 Microstructure of the deposited coatings close to (*a*) surface of the coating, (*b*) substrate surface, and (*c*) substrate material far from HAZ [130] (Reprinted with permission from Elsevier © 2011)

recrystallization in the friction surfacing process, the average Al grain size in the coating layer was smaller compared to the A6061 aluminum tool.

A smaller number of studies focused on the effect of different parameters on indirect measurements of strength and quality of the coating, most often by hardness measurements and view of the grain microstructure. Casalino et al. conducted an investigation on the effects of tool shoulder geometry and its deposition on the microstructure and microhardness of 5754H11 aluminum alloy plate with 3 mm thickness [84]. The microhardness profile and the grain size of the microstructural zones in the butt weld were measured. Shinoda et al. employed an approach that created a hard deposition layer with 1 mm thickness using friction surfacing [104]. Experimental analyses were performed to measure the effects of parameters in the process of depositing material. It was exhibited that the tool rotational speed had a significant influence on the hardness of the deposition. A harder deposition layer was formed when the rod had a lower rotational speed.

Kumar and Sammaiah enhanced the corrosion behavior of aluminum and steel by depositing zinc onto them [125]. Increasing friction during the process resulted in an increment in the zinc deposition onto mild steel and aluminum alloy. It was revealed that lower feed rate, higher rotational speed, and lower forward time produced smaller zinc crystalline size on the substrate. An investigation was carried out by Batchelor et al. to study different materials, deposition parameters, and the number of deposited layers [74]. In this study, aluminum, stainless steel, and brass as the consumable materials were coated onto mild carbon steel while nitrogen shielding gas was flowing over the surfaces. A strong thick coating layer was created on the stainless steel, but the approach was not successful for either aluminum or brass. The nitrogen flow reduced the deposition quality owing to the cooling effect on the coating tool and layer.

Li et al. investigated friction surfacing of AA5083 consumable rod on a DH36 steel substrate considering the effects of process parameters such as spindle speed, table travel speed, and feed rate on the friction depositions [75]. Optical microscopy, SEM, and EDS were utilized to evaluate the characteristics of the coating layers. The results of the experimental tests show that increment of the feed rate, travel speed, and axial force results in lower deposition surface quality. Also, a higher feed rate, higher rotational speed, and lower travel speed result in higher bond strength. The peak temperature occurs at the center of the deposition zone, and it was exhibited that a lower travel speed resulted in higher heat input per unit time and consequently at a higher temperature.

Rathee et al. studied the current trends, strategies, and issues in the fabrication process of surface composites using friction stir processing [161]. Their study paid special attention to important factors involved in the surface composite fabrication process, and the microstructural and mechanical characteristics corresponding to these factors. Govardhan et al. made an attempt to study the friction surfacing deposition of stainless steel over the surface of a low carbon steel substrate [105]. The effects of process parameters were investigated during the friction surfacing process of different combinations of materials, shear strength, and surface roughness.

Hanke et al. studied the friction surfaced coating of NiAl-bronze deposited onto self-mating substrates [130]. To study the wear resistance performance of the deposited surfaces, cavitation evaluation was conducted. The single-coating layer of NiAl-bronze onto the same substrate material exhibits a fine-grained and homogeneous microstructure. Resistance against cavitation erosion in the friction surfaced layers was superior to that found in cast material. In Fig. 29, the microstructures of the deposited sample at the areas close to the coating surface, substrate surface, and substrate material far from the heat-affected zone are presented.

The morphological and microstructural analyses on the friction deposition of AA2024 consumable rod onto the AA6061 substrate were investigated in Ref. [40]. During the friction surfacing process, the AA6061 substrate surface and the deposited AA2024 exhibit significant grain refinement due to the continuous dynamic recrystallization. The analysis exhibited an almost fully recrystallized microstructure in the deposited coating that was similar throughout

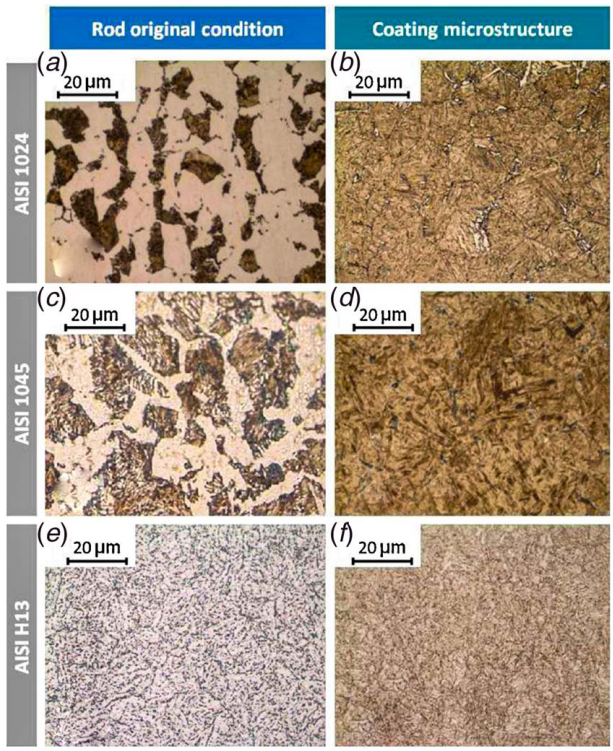

Fig. 30 Comparison between different consumable tool original condition and deposition coating microstructure [106] (Reprinted with permission from Elsevier © 2014)

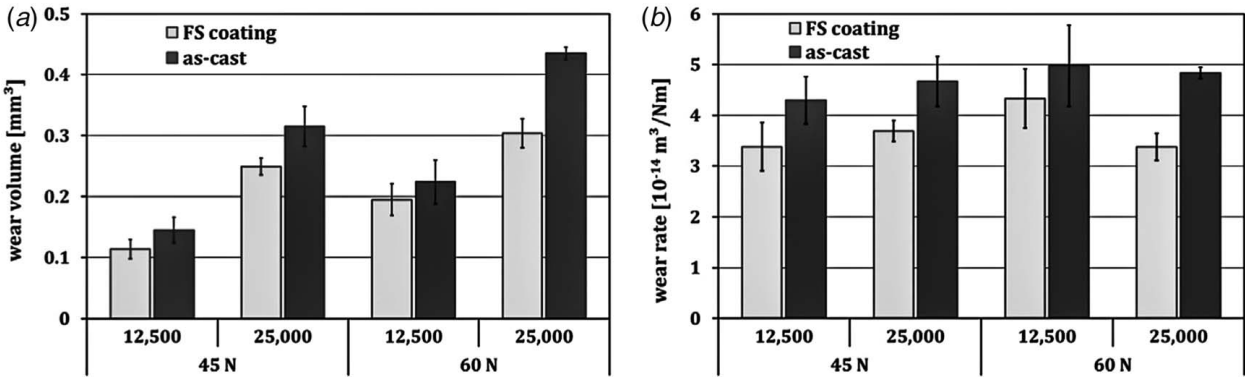

Fig. 31 (*a*) Wear volumes and (*b*) average wear-rates of the flats over normal force and number of cycles from ball-on-flat wear test [131] (Reprinted with permission from Elsevier © 2015)

the interfacial zones. This fact indicates that the entire deposited material experienced a similar thermomechanical history with severe deformation. The result revealed a partially recrystallized microstructure in the substrate with less deformation during the process.

A comparison between the microstructures of AISI 1024, AISI 1045, and AISI H13 deposits and the consumable materials as-received is presented by Pereira et al., as shown in Fig. 30 [106]. The martensitic and bainitic microstructures present in the deposit exhibit that the deposited coating was undergone full austenitization.

4.2 Wear and Corrosion Testing. Hanke et al. studied friction surfacing of Cr60Ni40 cast alloy on Nimonic 80A substrates [131]. The evolution of deposition's microstructures was examined and compared to the tool material microstructure in an as-cast state. A reciprocating ball-on-flat wear test was used, and the wear resistance performance of all deposition was slightly better than the as-received material, and the results of wear tests are shown in Fig. 31.

Sudherson et al. studied friction surfacing of aluminum alloy 5083-cadmium composite consumable rod onto AISI 1018 mild steel substrate in a corrosive environment using a modified lathe setup [76]. In this investigation, the friction surfaced samples were subjected to heat treatment evaluation at 100, 150, and 200 °C. Corrosion samples were produced and subjected to immersion in various solutions such as HCl, nitric acid, and $HClO_4$ for various corrosion evaluations, and the results were examined by using SEM and the weight loss method. The corrosion tests revealed that the friction surfaced samples have higher corrosion resistance than heat-treated friction surfaced samples and the mild steel substrate, as shown in Fig. 32(*a*). Therefore, at a particular pH value, the weight loss in mild steel was higher compared to coated and heat-treated coated specimens. Also, it was confirmed that weight loss decreased as the pH value increased. Figure 32(*b*) shows that the corrosion rate for all the samples increased as the number of hours of immersion increased.

Puli et al. investigated the coating of AISI 410 stainless steel on the surface of a mild steel substrate [107]. The deposited coatings exhibited martensitic microstructures with an average hardness value of 460 HV, which were very hard. Also, bend and shear tests exhibited results of excellent bonding between the coating and substrate. In another study, the friction surfacing of 440C stainless steel onto a low carbon steel substrate was examined by Puli and Ram [108]. Bend and shear tests on coating layers exhibited excellent bonding between the coating and substrate. The deposition showed superior corrosion resistance performance, while wear resistance performance was slightly inferior. Recently, stainless steel was friction surfaced on the surface of mild steel substrate by Nixon et al. [109]. The joint strength was examined by ram tensile testing, and the result exhibits a peak strength of 502 MPa for the coating layers. The corrosion resistance performance of the deposited layers was shown to be worse than that of the tool material, but better than for the substrate. Pereira et al. created a multilayer coating of AISI 1024, AISI 1045, and AISI H13 onto the substrate of mild steel [106]. The principal aim of this study was to determine which material combination provides more wear resistant. As shown in Fig. 33, AISI 1024 coating had the lowest wear friction coefficient and wear rate.

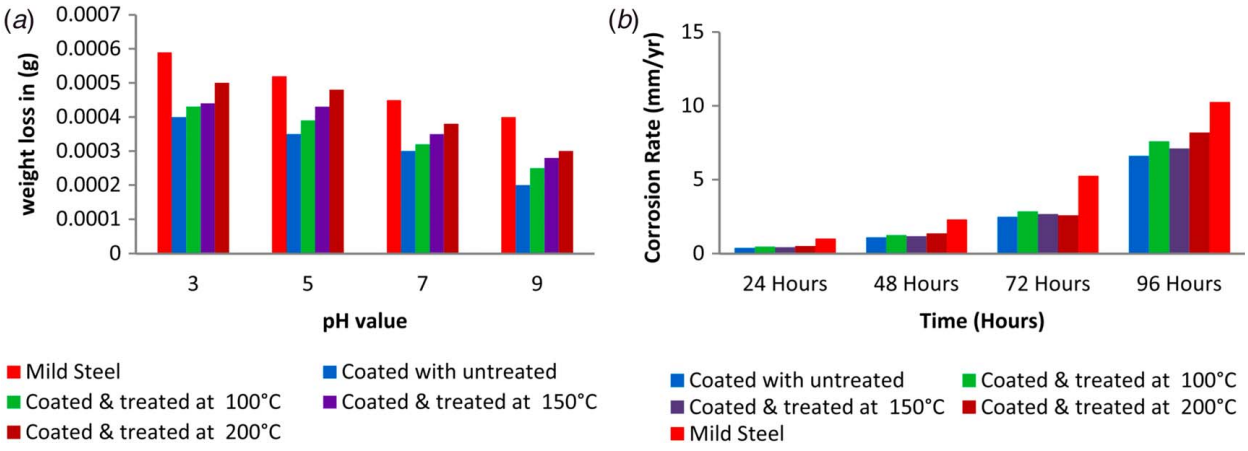

Fig. 32 (*a*) Weight loss versus various pH value and (*b*) corrosion rate versus number of hours [76] (Reprinted with permission from IOP Publishing, Ltd. © 2013)

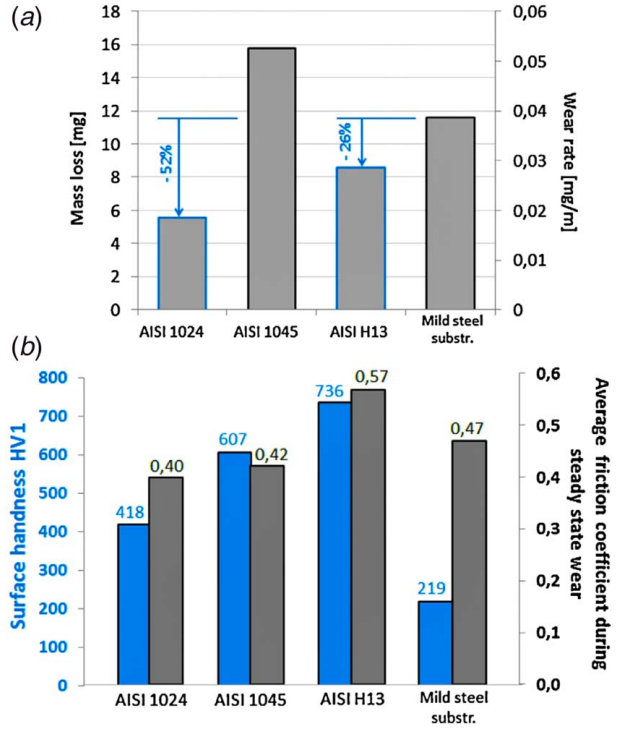

Fig. 33 (*a*) Mass loss measured by pin-on-disc wear evaluation technique and (*b*) surface hardness values and average of friction coefficient during steady-state wear [106] (Reprinted with permission from Elsevier © 2014)

In another investigation, the friction surfaced deposition of tool steel AISI H13 onto low carbon steel was studied by Rafi et al. [110]. Microstructural and microhardness tests were employed to evaluate the deposited coatings in detail, which revealed coating layers free from defects. The deposited coatings had a significantly higher hardness value (58 HRC) than the annealed consumable material (20 HRC). Singh et al. examined the friction surfacing of AISI 304 (austenitic stainless steel) as the consumable tool material over high-strength low alloy (HSLA) steel substrate [111]. The deposition and substrate were subjected to pitting corrosion examination by using the potentiodynamic polarization technique. The experimental result reveals that the coating layer shows less pitting resistance performance compared to the consumable material and higher than that of the HSLA substrate. In a different investigation, Rafi et al. exhibited that the friction surfaced deposition of AISI 304 shows higher corrosion resistance performance in many different environments [112].

In a recent investigation [113], Guo et al. successfully fiction surfaced precipitation hardened 17-4 *p*H Stainless Steel onto AISI 304 to improve the surface hardness. During the friction surfacing process, the originally existed incoherent precipitates (Cu and CrN) in the as-received consumable tool were re-dissolved into the deposit. During the operation, argon gas was utilized to protect the processing zone from surface oxidation. Increasing the tool rotational speed and traverse speed resulted in a decrement in the thickness and width of the coating. It was exhibited that due to the martensitic transformation, the processing parameters did not have any significant impacts on the hardness and microstructures of the deposited coating. In an investigation by Hanke Inconel alloy 625 (Ni-based alloy) was deposited onto 42CrMo4 steel alloy substrate, suitable for surface corrosion protection [124]. The results indicated that the dynamic recrystallization process and the thermal cycle define the final microstructure properties.

4.3 Mechanical Testing. Several studies have been carried out on the characterization of mechanical properties of aluminum alloys employed in the friction surfacing technique. Gandra et al. studied friction surfacing of AA6082-T6 onto AA2024-T3, considering bending, tensile, and wear characterization [22]. The deposition had 25% lower ultimate tensile strength than in the substrate material and the strain value was increased by 42% at break points. Figure 34 presents the hardness variation of the consumable

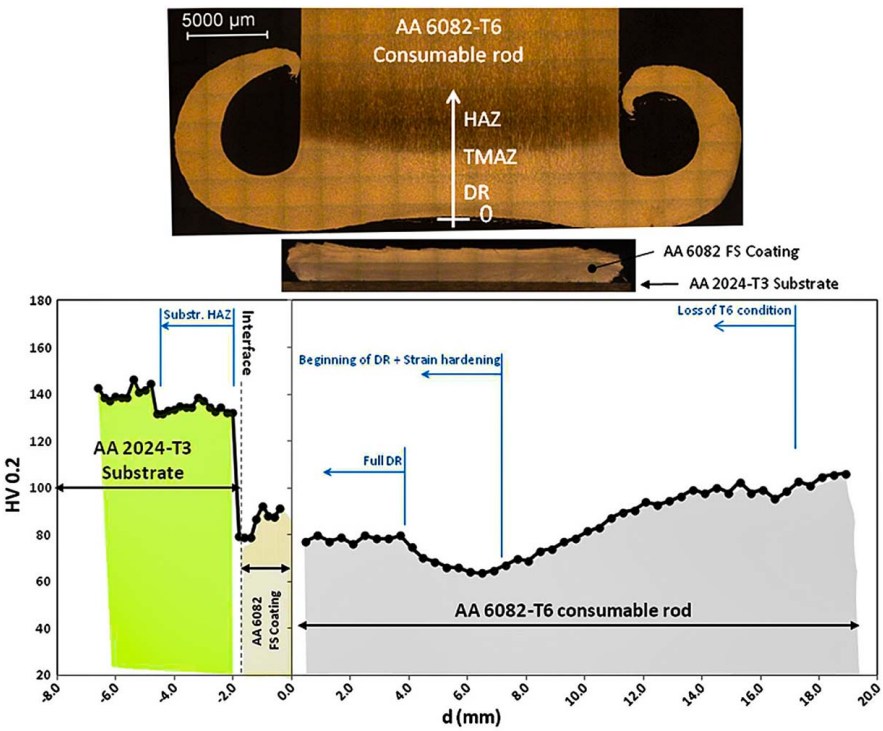

Fig. 34 Hardness profile along the consumable rod and the coating cross section [22] (Reprinted with permission from Elsevier © 2013)

tool and deposition cross section caused by the thermomechanical events during friction surfacing.

A commercially pure aluminum consumable rod was deposited onto medium carbon steel by Janakiraman and Bhat [77]. The result showed a consistent interface between the substrate and the deposited coating. An experimental setup was prepared by Stegmueller et al. to investigate relationships in the conventional friction surfacing process with inductive heating [85]. The result exhibits a very low mount of flash material generation as well as high-strength joint values in shear and push-off tests at tool rotational speed of 3000 rpm and pneumatic cylinder pressure of 8 bar. The stainless steel 1.4301 was friction surfaced onto AlMgSi0.5 aluminum alloy substrate by Stegmüller et al. [86]. It was proven that samples subjected to the inductive heating technique show higher shear strength in the deposited coating than those utilized flash-reducing tool method and classical process. Sahoo et al. [63] found that the highest push-off strength, surface hardness value, and bending strength were measured in deposition from the MF5 tool in Fig. 9, measured as 79.4 MPa, 137 HV, and 363 MPa, respectively.

Galvis et al. [41] investigated the double layer deposition of AA6351-T6 consumable rod onto AA5052-H32 substrate to assess the adhesion of the double-pass deposition on the substrate. Also, the influence of the surface roughness of the first layer on the deposition of the second layer was studied. Ravisekhar et al. confirmed that friction surfacing can be employed to produce deposition of dissimilar materials by using a vertical milling machine [78]. Many inspection methods including optical microscopy, SEM, and X-ray diffraction as well as techniques such as tensile testing, microstructural analysis, and hardness testing have been employed to evaluate the deposited coating quality.

In another investigation by Khalid Rafi et al. [114], the deposited coating layers of H13 tool steel and AISI 310 austenitic stainless steel onto mild steel substrates were completed to study wear and corrosion protection, respectively. The deposition was characterized by optical microscopy, SEM, shear tests, and bend tests. The H13 tool steel deposition was not strong in bending, and cracks appeared after five degrees of bending, which refers to the tool steel's inherent brittleness. On the other hand, the austenitic stainless steel deposition exhibited the bending ability up to 90 deg without any cracks.

5 Conclusions, Challenges, and Future Trends

This review shows that there is a growing body of friction stir processing literature related to friction surfacing by means of consumable tools. Material is transferred from the tool to the substrate for coating and similar/dissimilar material joining applications. Friction surfacing by a consumable tool has excellent capability to be employed as a means of dissimilar metal joining, a field of growing interest. This paper has been organized into three principal considerations of friction surfacing: different processing techniques, the influence of process factors on the quality of deposited coating, and lastly, the characterization, metallurgical and mechanical properties of the deposition. There are many investigations detailing the friction depositing technique with particular attention to the material transferring from a rotating rod enabled by high axial force and frictional heat. Further research and study are needed in the following categories.

5.1 Further Expansion of Materials, Variations of Processing Techniques, and Applications. The research trend is nascent with the majority of studies being experimental and metallurgical exploration in nature. The work to date suggests that there is still room for investigations using various combinations of material and reinforcement particles, coating quality, tool shapes, and consistency for the presented technique to be legitimately feasible in the industry. There are several investigations on process factors and different material combination used as the consumable tools and substrates. The various combinations of tool–substrate materials that have already been investigated were presented in Table 1. This table reveals that most of the researches have been focused on steel and aluminum alloys as both tool and substrate materials; however, there are many other industrial materials such as titanium, brass, zinc, Inconel, monel, magnesium, and stellite6 that have been utilized in quite a few studies. A deeper understanding and knowledge in this research area could be achieved only by developing friction deposits of various materials. There is a need to assess the possibility and quality of relevant material depositions, such as zinc-steel, monel-steel, and aluminum-copper, to have a better suggestion in industrial applications.

In the general field of friction stir processing since its invention, there have been a growing number of processing techniques, tool–workpiece configurations, and applications. Friction stir processing can now be used to weld, form, drill, modify surface properties, and now deposit material. In this review alone, there are different variations of friction surfacing described in the literature. It is anticipated that many more variations of the friction surfacing process will be studied and presented in the future. As the range of materials and tool configurations widens, so do the possible techniques and applications.

Most of the investigations in this review use the friction surfacing technique to provide friction deposition. It should be considered that the application of friction surfacing is not limited to creating coating layers. There are many other products that the friction surfacing technique could be used for. There are fewer investigations discussing different tool–workpiece configurations for depositing material for new purposes, such as joining dissimilar materials or keyhole filling. Therefore, friction surfacing could be extensively applied to add material for structural and joining purposes. Also, this technique should be studied to be considered for cavity filling purposes. Improving the corrosion resistance is another application for the friction surfacing method which lacks sufficient work in published literature. Moreover, this technique can be used in a multi-pass deposition process to create a multilayer composite part as was presented in Ref. [49].

There are several investigations on inserting reinforcing particles into the holes drilled along the length of the consumable tool to improve the mechanical properties on the deposited layers; however, there is a lack of studies focusing on the impacts of different types and percentage of reinforcing particles. As was discussed in Ref. [123], hole placement influences the efficiency of deposition, process behavior, coating quality, and particle distribution in the coating layer. Moreover, two different approaches of adding the reinforcing particles in drilled holes and the powder laying technique shows significant differences in the deposited coatings [51]. All these unanswered questions emphasize that more investigations on the influence of the different reinforcing particles and their percentage, different approaches, and configurations of applying particles are needed.

As this review research showed, most of the investigations have been focused on the conventional method of friction surfacing using a consumable rod; however, there are novel applications and approaches that require more developments. A novel method of friction surfacing (lateral friction surfacing) has been introduced and investigated in Refs. [15,79]. In this approach, the radial surface of a rotating consumable tool was forged against the substrate's surface while it moves across, and the deposit transfers from the side of the tool. There are many unknowns regarding different aspects of this technique and require various analyses to be revealed. Therefore, this study implies special attention to studying and developing novel methods and new applications in friction surfacing.

5.2 More Comprehensive Understanding and Control of Material Transferring Process. There is a need to gain an in-depth understanding of the friction surfacing technique and the mechanism of the material transferring process on the micro

scales to control it appropriately. This is a technique with a growing number of applications, but there are still many questions and lack of knowledge in many parts of this process, specifically about the conditions for material transfer from consumable tool to substrate. There have been many experimental investigations on process parameters and materials, but these have resulted in causal relationships without insight into the underlying mechanisms for material transfer from the tool to substrate. If the conditions of stress, strain, and temperature at the point of transfer can be fully quantified and understood, the process can be more accurately simulated with FEM. As shown in Table 3, there is not a clear trend of the effect of process parameters on the nature of deposition. A deeper understanding of this process is necessary to address all the processing challenges from theoretical and practical aspects.

The advance of analysis techniques and tools is important for a deeper understanding of the physics of friction surfacing. This includes a need to develop accurate finite element techniques to investigate the distribution of stress, strain, and temperature throughout the tool coating, and substrate during the process. The FEM code has been investigated for friction stir welding and friction stir processes where the tool and workpiece remain separate. There have been a couple of studies with FEM [31–33,35], but this area has much room for expansion. Stress can be calculated for different coating-substrate systems which results in various values of Young's modulus ratio, coating thickness, and friction coefficient. During the deposition, it is essential to analyze the residual stresses generated in the product. Also, computer modeling using the finite element method can be adapted to study the wear mechanism and simulate the wear profile of the deposition.

In the fusion welding processes, there is a need to prevent the heated area from the oxidizing effect of the ambient atmosphere. The friction surfacing process produces different temperatures based on the employed process parameters and materials. A suitable shielding gas can successfully provide the required protection for the heat-affected zone. On the other hand, the shielding gas can affect the microstructure of the processing zone, material transferring process, and heat transferring process by providing forced convection. There are only a few investigations in friction surfacing in which a shielding gas has been utilized [74,100], and there is no investigation to address the detailed impacts of shielding gas on the friction depositing process. The shielding gas composition and the gas flow rate are the imperative factors during operation, and their impacts on the deposited coating and the material transferring process should be addressed in future researches.

5.3 Full Quantification of the Influences of Process Factors on Deposition Quality and Process Scale Up. To achieve a coating layer with fine grain size, low residual stress, low porosity, and high level of hardness, all the affecting process parameters should be studied. Most of the accomplished investigations are only focused on few process parameters such as tool rotational speed, axial force, and table traverse speed. However, there are various process parameters, which can significantly affect the quality of the deposition process that has not been fully studied. For instance, the diameter of the rod, friction coefficient value between the rod and substrate, pre-heating process and initial temperature of the tool–substrate, and cooling down rate are the factors that might have a significant influence on the result.

In the refill friction stir spot welding process using friction surfacing technique, the working part of the tool consists of the pin (penetrating part) and shoulder, and their dimensions such as height and diameter of the shoulder and consumable pin, and the inclination angle of shoulder tip surface play a significant role in the resulting material transfer. There are just a few investigations regarding the influences of tool shape (profiles) in friction surfacing processes.

Moreover, flash formation is a critical issue in the friction surfacing process that can waste 40–60% of the total consumable material, as discussed in Ref. [21]. Moreover, the secondary flash grows on the consumable rod parallel to the substrate surface and has this capability of affecting the coated deposit. Despite the high importance of these issues, there are only a few investigations with attention to the flash formation during the friction surfacing. More investigations are required to understand the difference between primary and secondary flashes and reasons that cause each one. There is a need to deeply understand the influential process parameters affecting on the formation of primary and secondary flashes, to provide the capability of preventing this issue. More investigation about the effects of each factor will result in a better control system to achieve the best quality and maximum efficiency. Also, by studying the ways to automate the processes, high volume production on an industrial scale could be achieved.

Credit Author Statement

Ebrahim Seidi: Conceptualization, Data Curation, Formal Analysis, Investigation, Visualization, Writing—Original Draft Preparation, Writing—Review and Editing.

Scott F. Miller: Funding Acquisition, Writing—Original Draft Preparation, Writing—Reviewing and Editing, Supervision.

Blair E. Carlson: Writing—Reviewing and Editing.

Acknowledgment

We acknowledge the support from General Motors and NSF CMMI (Grant No. 1763147).

Conflict of Interest

There are no conflicts of interest.

Data Availability Statement

No data, models, or code were generated or used for this paper.

References

[1] Cai, W., Daehn, G., Vivek, A., Li, J., Khan, H., Mishra, R. S., and Komarasamy, M., 2019, "A State-of-the-Art Review on Solid-State Metal Joining," ASME J. Manuf. Sci. Eng., **141**(3), p. 031012.
[2] Klopstock, H., and Neelands, A. R., 1941, "An Improved Method of Joining or Welding Metals," UK Patent No. GB572789.
[3] Gandra, J., Krohn, H., Miranda, R. M., Vilaça, P., Quintino, L., and Dos Santos, J. F., 2014, "Friction Surfacing—A Review," J. Mater. Process. Technol., **214**(5), pp. 1062–1093.
[4] Jambhale, S., Kumar, S., and Kumar, S., 2015, "Effect of Process Parameters & Tool Geometries on Properties of Friction Stir Spot Welds: A Review," Univ. J. Eng. Sci., **3**(1), pp. 6–11.
[5] Ojo, O. O., Taban, E., and Kaluc, E., 2015, "Friction Stir Spot Welding of Aluminum Alloys: A Recent Review," Mater. Test., **57**(7–8), pp. 609–627.
[6] Yang, X. W., Fu, T., and Li, W. Y., 2014, "Friction Stir Spot Welding: A Review on Joint Macro-and Microstructure, Property, and Process Modelling," Adv. Mater. Sci. Eng., **2014**, pp. 1–11.
[7] Pan, T. Y., 2007, "Friction Stir Spot Welding (FSSW)—A Literature Review," SAE World Congress & Exhibition, SAE Technical Paper No. 2007-01-1702.
[8] Avettand-Fènoël, M. N., and Simar, A., 2016, "A Review About Friction Stir Welding of Metal Matrix Composites," Mater. Charact., **120**, pp. 1–17.
[9] Zhang, Y. N., Cao, X., Larose, S., and Wanjara, P., 2012, "Review of Tools for Friction Stir Welding and Processing," Can. Metall. Q., **51**(3), pp. 250–261.
[10] El-Bahloul, S. A., El-Shourbagy, H. E., Al-Makky, M. Y., and El-Midany, T. T., 2013, "Thermal Friction Drilling: (A Review)," Aerosp. Sci. Aviat. Technol., **15**(26), pp. 1–15.
[11] Sharma, V., Prakash, U., and Kumar, B. V. M., 2015, "Surface Composites by Friction Stir Processing: A Review," J. Mater. Process. Technol., **224**, pp. 117–134.
[12] Kumar, K., Gulati, P., Gupta, A., and Shukla, D. K., 2017, "A Review of Friction Stir Processing of Aluminium Alloys Using Different Types of Reinforcements," Int. J. Mech. Eng. Technol, **8**(7), pp. 1638–1651.
[13] Gangil, N., Siddiquee, A. N., and Maheshwari, S., 2017, "Aluminium Based In-Situ Composite Fabrication Through Friction Stir Processing: A Review," J. Alloys Compd., **715**, pp. 91–104.
[14] Ma, Z. Y., 2008, "Friction Stir Processing Technology: A Review," Metall. Mater. Trans. A, **39**(3), pp. 642–658.
[15] Seidi, E., and Miller, S. F., 2020, "A Novel Approach to Friction Surfacing: Experimental Analysis of Deposition From Radial Surface of a Consumable Tool," Coatings, **10**(11), p. 1016.

[16] Kumar, S., 2020, "Other Solid Deposition Processes," *Additive Manufacturing Processes*, Springer, New York, pp. 111–130.
[17] Seidi, E., and Miller, S. F., 2019, "Friction Surfacing Using Consumable Tools: A Review," Proceedings of the ASME 2019 14th International Manufacturing Science and Engineering Conference. Volume 2: Processes; Materials, Erie, PA, June 10–14, p. V002T03A048.
[18] Guo, D., Kwok, C. T., and Chan, S. L. I., 2019, "Spindle Speed in Friction Surfacing of 316L Stainless Steel—How It Affects the Microstructure, Hardness and Pitting Corrosion Resistance," Surf. Coat. Technol., **361**, pp. 324–341.
[19] Vilaça, P., Hänninen, H., Saukkonen, T., and Miranda, R. M., 2014, "Differences Between Secondary and Primary Flash Formation on Coating of HSS With AISI 316 Using Friction Surfacing," Weld. World, **58**(5), pp. 661–671.
[20] Liu, X. M., Zou, Z. D., Zhang, Y. H., Qu, S. Y., and Wang, X. H., 2008, "Figuration Control of Deposit in Friction Surfacing," Key Eng. Mater., **373–374**, pp. 806–810.
[21] Gandra, J., Miranda, R. M., and Vilaça, P., 2012, "Performance Analysis of Friction Surfacing," J. Mater. Process. Technol., **212**(8), pp. 1676–1686.
[22] Gandra, J., Pereira, D., Miranda, R. M., Silva, R. J. C., and Vilaça, P., 2013, "Deposition of AA6082-T6 Over AA2024-T3 by Friction Surfacing-Mechanical and Wear Characterization," Surf. Coat. Technol., **223**, pp. 32–40.
[23] Isupov, F. Y., Panchenko, O. V., Naumov, A. A., Alekseeva, M. D., Zhabrev, L. A., and Popovich, A. A., 2019, "Consumable Tool for Coating Deposition by Joint Deformation of the Base and Tool Materials," Russ. Metall., **2019**(13), pp. 1399–1406.
[24] Tosun, G., Ozler, L., and Ozcan, M. E., 2020, "Gradient Composite Coatings on AA5754 Using Friction Stir Process," Surf. Eng., **36**(5), pp. 447–455.
[25] Reddy, G. M., Rao, K. S., and Mohandas, T., 2009, "Friction Surfacing: Novel Technique for Metal Matrix Composite Coating on Aluminium–Silicon Alloy," Surf. Eng., **25**(1), pp. 25–30.
[26] Pirhayati, P., and Aval, H. J., 2019, "Effect of Silver on Non-Isothermal Aging of Friction Surfaced AA2024–16 wt% Ag Composites," Surf. Coat. Technol., **379**, p. 125059.
[27] Pirhayati, P., and Aval, H. J., 2020, "Effect of Post-Heat Treatment on Friction Surfaced Al-Cu-Mg Alloy Coating Containing Ag," Surf. Coat. Technol., **397**, p. 125984.
[28] Galvis, J. C., Oliveira, P. H. F., Hupalo, M. F., Martins, J. P., and Carvalho, A. L. M., 2017, "Influence of Friction Surfacing Process Parameters to Deposit AA6351-T6 Over AA5052-H32 Using Conventional Milling Machine," J. Mater. Process. Technol., **245**, pp. 91–105.
[29] Gandra, J., Pereira, D., Miranda, R. M., and Vilaça, P., 2013, "Influence of Process Parameters in the Friction Surfacing of AA 6082-T6 Over AA 2024-T3," Procedia CIRP, **7**, pp. 341–346.
[30] Kallien, Z., Rath, L., Roos, A., and Klusemann, B., 2020, "Experimentally Established Correlation of Friction Surfacing Process Temperature and Deposit Geometry," Surf. Coat. Technol., **397**, p. 126040.
[31] Pirhayati, P., and Aval, H. J., 2019, "An Investigation on Thermo-Mechanical and Microstructural Issues in Friction Surfacing of Al–Cu Aluminum Alloys," Mater. Res. Express, **6**(5), p. 056550.
[32] Bararpour, S. M., Aval, H. J., and Jamaati, R., 2019, "Modeling and Experimental Investigation on Friction Surfacing of Aluminum Alloys," J. Alloys Compd., **805**, pp. 57–68.
[33] Bararpour, S. M., Aval, H. J., and Jamaati, R., 2020, "An Experimental and Theoretical Investigation of Thermo-Mechanical Issues in Friction Surfacing of Al–Mg Aluminum Alloys: Material Flow and Residual Stress," Modell. Simul. Mater. Sci. Eng., **28**(3), p. 035003.
[34] Rahmati, Z., Aval, H. J., Nourouzi, S., and Jamaati, R., 2020, "Microstructural, Tribological, and Texture Analysis of Friction Surfaced Al-Mg-Cu Clad on AA1050 Alloy," Surf. Coat. Technol., **397**, p. 125980.
[35] Rahmati, Z., Aval, H. J., Nourouzi, S., and Jamaati, R., 2019, "Modeling and Experimental Study of Friction Surfacing of AA2024 Alloy Over AA1050 Plates," Mater. Res. Express, **6**(8), p. 0865g2.
[36] Dilip, J. J. S., and Ram, G. J., 2013, "Microstructure Evolution in Aluminum Alloy AA 2014 During Multi-Layer Friction Deposition," Mater. Charact., **86**, pp. 146–151.
[37] Suhuddin, U., Mironov, S., Krohn, H., Beyer, M., and Dos Santos, J. F., 2012, "Microstructural Evolution During Friction Surfacing of Dissimilar Aluminum Alloys," Metall. Mater. Trans. A, **43**(13), pp. 5224–5231.
[38] Tokisue, H., Katoh, K., Asahina, T., and Usiyama, T., 2006, "Mechanical Properties of 5052/2017 Dissimilar Aluminum Alloys Deposit by Friction Surfacing," Mater. Trans., **47**(3), pp. 874–882.
[39] Phillips, B. J., Avery, D. Z., Liu, T., Rodriguez, O. L., Mason, C. J. T., Jordon, J. B., Brewer, L. N., and Allison, P. G., 2019, "Microstructure-Deformation Relationship of Additive Friction Stir-Deposition Al–Mg–Si," Materialia, **7**, p. 100387.
[40] Perry, M. E., Griffiths, R. J., Garcia, D., Sietins, J. M., Zhu, Y., and Hang, Z. Y., 2020, "Morphological and Microstructural Investigation of the Non-Planar Interface Formed in Solid-State Metal Additive Manufacturing by Additive Friction Stir Deposition," Addit. Manuf., **35**, p. 101293.
[41] Galvis, J. C., Oliveira, P. H. F., Martins, J. D. P., and Carvalho, A. L. M. D., 2018, "Assessment of Process Parameters by Friction Surfacing on the Double Layer Deposition," Mater. Res., **21**(3), p. e20180051.
[42] Ehrich, J., Roos, A., and Hanke, S., 2019, "Effect of Mg and Si Content in Aluminum Alloys on Friction Surfacing Processing Behavior," *Light Metals 2019*, Springer International Publishing, pp. 357–363.
[43] Bararpour, S. M., Aval, H. J., and Jamaati, R., 2019, "Mechanical Alloying by Friction Surfacing Process," Mater. Lett., **254**, pp. 394–397.
[44] Bararpour, S. M., Aval, H. J., and Jamaati, R., 2020, "Effect of Non-Isothermal Aging on Microstructure and Mechanical Properties of Friction Surfaced AA5083-15wt% Zn Composites," Surf. Coat. Technol., **384**, p. 125307.
[45] Bararpour, S. M., Aval, H. J., and Jamaati, R., 2020, "Effects of Zn Powder on Alloying During Friction Surfacing of Al–Mg Alloy," J. Alloys Compd., **818**, p. 152823.
[46] Oliveira, P. H. F., Galvis, J. C., Martins, J. D. P., and Carvalho, A. L. M., 2017, "Application of Friction Surfacing to the Production of Aluminum Coatings Reinforced With Al2O3 Particles," Mater. Res., **20**(supl. 2), pp. 603–620.
[47] Pirhayati, P., and Aval, H. J., 2020, "Microstructural Characterization and Mechanical Properties of Friction Surfaced AA2024−Ag Composites," Trans. Nonferrous Met. Soc. China, **30**(7), pp. 1756–1770.
[48] Miranda, R. M., Santos, T. G., Gandra, J., Lopes, N., and Silva, R. J. C., 2013, "Reinforcement Strategies for Producing Functionally Graded Materials by Friction Stir Processing in Aluminium Alloys," J. Mater. Process. Technol., **213**(9), pp. 1609–1615.
[49] Karthik, G. M., Ram, G. J., and Kottada, R. S., 2016, "Friction Deposition of Titanium Particle Reinforced Aluminum Matrix Composites," Mater. Sci. Eng. A, **653**, pp. 71–83.
[50] Mohanasundaram, S., Vijay, S. J., Vasanth, X. A., Rai, R. S., and Kantharaj, I., 2020, "Optimization of Coating Thickness and Coating Width for Friction Surfaced Al6061-B_4C Over Al6061," Mater. Today: Proc., **33**(1), pp. 1–7.
[51] Özler, L., Tosun, G., and Özcan, M. E., 2020, "Influence of B4C Powder Reinforcement on Coating Structure, Microhardness and Wear in Friction Surfacing," Mater. Manuf. Processes, **35**(10), pp. 1135–1145.
[52] Sharma, A., Tripathi, A., Narsimhachary, D., Mahto, R. P., and Paul, J., 2019, "Surface Alteration of Aluminium Alloy by an Exfoliated Graphitic Tribolayer During Friction Surfacing Using a Consumable Graphite Rich Tool," Surf. Topogr. Metrol. Prop., **7**(4), p. 045015.
[53] Esther, I., Dinaharan, I., and Murugan, N., 2019, "Microstructure and Wear Characterization of AA2124/4wt% B_4C Nano-Composite Coating on Ti−6Al −4V Alloy Using Friction Surfacing," Trans. Nonferrous Met. Soc. China, **29**(6), pp. 1263–1274.
[54] Sharma, A., Sagar, S., Mahto, R. P., Sahoo, B., Pal, S. K., and Paul, J., 2018, "Surface Modification of Al6061 by Graphene Impregnation Through a Powder Metallurgy Assisted Friction Surfacing," Surf. Coat. Technol., **337**, pp. 12–23.
[55] Huang, Y. X., Han, B., Tian, Y., Liu, H. J., Lv, S. X., Feng, J. C., Leng, J. S., and Li, Y., 2011, "New Technique of Filling Friction Stir Welding," Sci. Technol. Weld. Joining, **16**(6), pp. 497–501.
[56] Huang, Y. X., Han, B., Lv, S. X., Feng, J. C., Liu, H. J., Leng, J. S., and Li, Y., 2012, "Interface Behaviours and Mechanical Properties of Filling Friction Stir Weld Joining AA 2219," Sci. Technol. Weld. Joining, **17**(3), pp. 225–230.
[57] Han, B., Huang, Y., Lv, S., Wan, L., Feng, J., and Fu, G., 2013, "AA7075 Bit for Repairing AA2219 Keyhole by Filling Friction Stir Welding," Mater. Des., **51**, pp. 25–33.
[58] Shen, Z., Chen, Y., Hou, J. S. C., Yang, X., and Gerlich, A. P., 2015, "Influence of Processing Parameters on Microstructure and Mechanical Performance of Refill Friction Stir Spot Welded 7075-T6 Aluminium Alloy," Sci. Technol. Weld. Joining, **20**(1), pp. 48–57.
[59] Pandya, S. N., and Menghani, J. V., 2018, "Developments of Mathematical Models for Prediction of Tensile Properties of Dissimilar AA6061-T6 to Cu Welds Prepared by Friction Stir Welding Process Using Zn Interlayer," Sādhanā, **43**(10), p. 168.
[60] Chandrasekaran, M., Batchelor, A. W., and Jana, S., 1997, "Friction Surfacing of Metal Coatings on Steel and Aluminum Substrate," J. Mater. Process. Technol., **72**(3), pp. 446–452.
[61] Badheka, K., and Badheka, V., 2017, "Friction Surfacing of Aluminium on Steel: An Experimental Approach," Mater. Today: Proc., **4**(9), pp. 9937–9941.
[62] Da Silva, M. M., Afonso, M. L. B., Silva, S. L. N., Troysi, F. C. T. D., Dos Santos, ÍB, and Brito, P. P., 2018, "Application of the Friction Surfacing Process in a CNC Machining Center: A Viability Assessment for Producing Al-Alloy Coatings on Low Carbon Steel," J. Braz. Soc. Mech. Sci. Eng., **40**(1), pp. 14–25.
[63] Sahoo, D. K., Mohanty, B. S., and Maalika Veetil, A. P., 2020, "Evaluation of Bond Strength and Flash Mass on Friction Surfaced Deposition of Aluminium 6063 Over IS 2062 Low Carbon Steel Using Different Mechtrode Face," Ann. Chim., **44**(2), pp. 109–119.
[64] Badheka, K., and Badheka, V. J., 2019, "Wear Behaviour of Boron Carbide Added Friction Surfaced Cladded Layer," *Innovations in Infrastructure. Advances in Intelligent Systems and Computing, 757*, D. Deb, V. Balas, and R. Dey, eds., Springer, Singapore, pp. 395–406.
[65] Sugandhi, V., and Ravishankar, V., 2012, "Optimization of Friction Surfacing Process Parameters for aa1100 Aluminum Alloy Coating With Mild Steel Substrate Using Response Surface Methodology (RSM) Technique," Mod. Appl. Sci., **6**(2), pp. 69–80.
[66] Sahoo, D. K., and Mohanty, B. S., 2019, "Evaluation of Bond Strength on Deposition of Aluminium 6063 Alloy Over EN24 Medium Carbon Steel by Friction Surfacing Using Different Mechtrode Diameter," e-J. Surf. Sci. Nanotechnol., **17**, pp. 83–94.
[67] Sahoo, D. K., Mohanty, B. S., Pradeep, A. M., and John, A. D. F., 2020, "An Experimental Study on Friction Surfaced Coating of Aluminium 6063 Over AISI 316 Stainless Steel Substrate," Mater. Today: Proc., **40**(1), pp. 1–9.
[68] Sahoo, D. K., Mohanty, B. S., and Echempati, R., 2020, "Computation of Roughness at Substrate Coating Interface on Deposition of Aluminium Over Medium Carbon Steel by Friction Surfacing," Dig. J. Nanomater. Biostruct., **15**(2), pp. 513–526.

[69] Kumar, B. V., Reddy, G. M., and Mohandas, T., 2015, "Influence of Process Parameters on Physical Dimensions of AA6063 Aluminium Alloy Coating on Mild Steel in Friction Surfacing," Def. Technol., **11**(3), pp. 275–281.
[70] Vasanth, R., Mohan, K., Rengarajan, S., Jayaprakash, R., and Kumar, R. A., 2019, "Characterization and Corrosion Effects of Friction Surfaced IS-2062 E250 CU With AA6063," Mater. Res. Express, **6**(12), p. 126579.
[71] Kumar, B. V., Reddy, G. M., and Mohandas, T., 2014, "Identification of Suitable Process Parameters for Friction Surfacing of Mild Steel With AA6063 Aluminium Alloy," Int. J. Adv. Manuf. Technol., **74**(1–4), pp. 433–443.
[72] Sahoo, D. K., Chari, A. N., and Reddy, A. S., 2019, "Optimization & Characterization of Friction Surfaced Coatings of AA6063 Aluminium Alloy Over AISI316 Stainless Steel Substrate," Mater. Today: Proc., **23**(3), pp. 1–8.
[73] Yu, M., Zhang, Z., Zhao, H., Zhou, L., and Song, X., 2019, "Microstructure and Corrosion Behavior of the Ultra-Fine Grained Aluminum Coating Fabricated by Friction Surfacing," Mater. Lett., **250**, pp. 174–177.
[74] Batchelor, A. W., Jana, S., Koh, C. P., and Tan, C. S., 1996, "The Effect of Metal Type and Multi-Layering on Friction Surfacing," J. Mater. Process. Technol., **57**(1–2), pp. 172–181.
[75] Li, H., Qin, W., Galloway, A., and Toumpis, A., 2019, "Friction Surfacing of Aluminium Alloy 5083 on DH36 Steel Plate," Metals, **9**(4), p. 479.
[76] Sudherson, D. P. S., Anandkumar, P. P., Jinu, G. R., Balasubramanian, K. A., and Vettivel, S. C., 2019, "Experimental Investigation on Corrosion Behavior of Friction Surfaced Mild Steel With Aluminum Alloy 5083-Cadmium Composite," Mater. Res. Express, **6**(8), p. 086587.
[77] Janakiraman, S., and Bhat, K. U., 2012, "Formation of Composite Surface During Friction Surfacing of Steel With Aluminium," Adv. Tribol., **2012**, p. 614278.
[78] Ravisekhar, S., Das, V. C., and Govardhan, D., 2017, "Friction Surfaced Deposits for Industrial Applications," Mater. Today: Proc., **4**(2), pp. 3796–3801.
[79] Seidi, E., and Miller, S. F., 2020, "Friction Surfacing From Radial Surface of A6063 Aluminum Alloy Consumable Tool Onto A36 Carbon Steel," Proceedings of the ASME 2020 International Mechanical Engineering Congress and Exposition, Volume 2A: Advanced Manufacturing, Virtual, Online, Nov. 16–19, p. V02AT02A003.
[80] Miles, M. P., Kohkonen, K., Packer, S., Steel, R., Siemssen, B., and Sato, Y. S., 2009, "Solid State Spot Joining of Sheet Materials Using Consumable Bit," Sci. Technol. Weld. Joining, **14**(1), pp. 72–77.
[81] Miles, M. P., Feng, Z., Kohkonen, K., Weickum, B., Steel, R., and Lev, L., 2010, "Spot Joining of AA 5754 and High Strength Steel Sheets by Consumable Bit," Sci. Technol. Weld. Joining, **15**(4), pp. 325–330.
[82] Stegmüller, M. J., Grant, R. J., and Schindele, P., 2019, "Quantification of the Interfacial Roughness When Coating Stainless Steel Onto Aluminium by Friction Surfacing," Surf. Coat. Technol., **375**, pp. 22–33.
[83] Shariq, M., Srivastava, M., Tripathi, R., Chattopadhyaya, S., and Dixit, A. R., 2016, "Feasibility Study of Friction Surfaced Coatings Over Non-Ferrous Substrates," Procedia Eng., **149**, pp. 465–471.
[84] Casalino, G., Campanelli, S., and Mortello, M., 2014, "Influence of Shoulder Geometry and Coating of the Tool on the Friction Stir Welding of Aluminium Alloy Plates," Procedia Eng, **69**, pp. 1541–1548.
[85] Stegmueller, M. J. R., Schindele, P., and Grant, R. J., 2015, "Inductive Heating Effects on Friction Surfacing of Stainless Steel Onto an Aluminium Substrate," J. Mater. Process. Technol., **216**, pp. 430–439.
[86] Stegmüller, M. J., Grant, R. J., and Schindele, P., 2019, "Improvements in the Process Efficiency and Bond Strength When Friction Surfacing Stainless Steel Onto Aluminium Substrates," Proc. Inst. Mech. Eng., Part L, **233**(4), pp. 687–698.
[87] Nixon, R., and Mohanty, B. S., 2013, "Friction Surfacing of Metal Coatings on Stainless Steel AISI 304 Over Spheroidal Graphite Iron Substrate," *Advanced Materials Research*, A. Ghanbari, ed., Trans Tech Publications Ltd, Vol. 816–817, pp. 271–275.
[88] Kramer de Macedo, M. L., Pinheiro, G. A., dos Santos, J. F., and Strohaecker, T. R., 2010, "Deposit by Friction Surfacing and Its Applications," Weld. Int., **24**(6), pp. 422–431.
[89] Troysi, F., Silva, K., Santos, ÍD, and Brito, P., 2019, "Investigation of Austenitic Stainless Steel Coatings on Mild Steel Produced by Friction Surfacing Using a Conventional CNC Machining Center," Mater. Res., **22**(2), p. e20180301.
[90] Rao, K. P., Sreenu, A. V., Rafi, H. K., Libin, M. N., and Balasubramaniam, K., 2012, "Tool Steel and Copper Coatings by Friction Surfacing—A Thermography Study," J. Mater. Process. Technol., **212**(2), pp. 402–407.
[91] Liu, X. M., Zou, Z. D., Zhang, Y. H., Qu, S. Y., and Wang, X. H., 2008, "Transferring Mechanism of the Coating Rod in Friction Surfacing," Surf. Coat. Technol., **202**(9), pp. 1889–1894.
[92] Dilip, J. J. S., Babu, S., Rajan, S. V., Rafi, K. H., Ram, G. J., and Stucker, B. E., 2013, "Use of Friction Surfacing for Additive Manufacturing," Mater. Manuf. Processes, **28**(2), pp. 189–194.
[93] Vitanov, V. I., and Voutchkov, I. I., 2005, "Process Parameters Selection for Friction Surfacing Applications Using Intelligent Decision Support," J. Mater. Process. Technol., **159**(1), pp. 27–32.
[94] Nixon, R. G. S., Mohanty, B. S., and Bhaskar, G. B., 2018, "Effect of Process Parameters on Physical Measurements of AISI316 Stainless Steel Coating on EN24 in Friction Surfacing," Mater. Manuf. Processes, **33**(7), pp. 778–785.
[95] Sahoo, D. K., Pradeep, A. M., Mohanty, B. S., and Jaswanth, A., 2020, "Influence of Inductive Heating on Coating Geometry During Deposition of AISI 316 Stainless Steel Over EN8 Carbon Steel Using Friction Surfacing Process," Mater. Today: Proc., **27**(2), pp. 1–10.
[96] Sahoo, D. K., Mohanty, B. S., John, D. F., and Pradeep, A. M., 2020, "Multi Response Optimization and Desirability Function Analysis on Friction Surfaced Deposition of AISI 316 Stainless Steel Over EN8 Medium Carbon Steel," Mater. Today: Proc., **40**(1), pp. 1–9.
[97] Rafi, H. K., Ram, G. J., Phanikumar, G., and Rao, K. P., 2010, "Friction Surfaced Tool Steel (H13) Coatings on Low Carbon Steel: A Study on the Effects of Process Parameters on Coating Characteristics and Integrity," Surf. Coat. Technol., **205**(1), pp. 232–242.
[98] Silva, K. H. S., Brito, P. P., Santos, I. B., Câmara, M. A., and Abrão, A. M., 2020, "The Behaviour of AISI 4340 Steel Coatings on Low Carbon Steel Substrate Produced by Friction Surfacing," Surf. Coat. Technol., **399**, p. 126170.
[99] Sekharbabu, R., Rafi, H. K., and Rao, K. P., 2013, "Characterization of D2 Tool Steel Friction Surfaced Coatings Over Low Carbon Steel," Mater. Des., **50**, pp. 543–550.
[100] Guo, D., Kwok, C. T., and Chan, S. L. I., 2019, "Strengthened Forced Convection—A Novel Method for Improving the Pitting Corrosion Resistance of Friction-Surfaced Stainless Steel Coating," Mater. Des., **182**, p. 108037.
[101] Govardhan, D., Kumar, A. C. S., Murti, K. G. K., and Reddy, G. M., 2012, "Characterization of Austenitic Stainless Steel Friction Surfaced Deposit Over Low Carbon Steel," Mater. Des., **36**, pp. 206–214.
[102] Puli, R., and Ram, G. J., 2012, "Dynamic Recrystallization in Friction Surfaced Austenitic Stainless Steel Coatings," Mater. Charact., **74**, pp. 49–54.
[103] Puli, R., and Ram, G. J., 2012, "Wear and Corrosion Performance of AISI 410 Martensitic Stainless Steel Coatings Produced Using Friction Surfacing and Manual Metal Arc Welding," Surf. Coat. Technol., **209**, pp. 1–7.
[104] Shinoda, T., Li, J. Q., Katoh, Y., and Yashiro, T., 1998, "Effect of Process Parameters During Friction Coating on Properties of Non-Dilution Coating Layers," Surf. Eng., **14**(3), pp. 211–216.
[105] Govardhan, D., Sammaiah, K., Murti, K. G. K., and Reddy, G. M., 2015, "Evaluation of Bond Quality for Stainless Steel-Carbon Steel Friction Surfaced Deposits," Mater. Today: Proc., **2**(4–5), pp. 3511–3519.
[106] Pereira, D., Gandra, J., Pamies-Teixeira, J., Miranda, R. M., and Vilaça, P., 2014, "Wear Behaviour of Steel Coatings Produced by Friction Surfacing," J. Mater. Process. Technol., **214**(12), pp. 2858–2868.
[107] Puli, R., Kumar, E. N., and Ram, G. J., 2011, "Characterization of Friction Surfaced Martensitic Stainless Steel (AISI 410) Coatings," Trans. Indian Inst. Met., **64**(1–2), p. 41.
[108] Puli, R., and Ram, G. J., 2012, "Microstructures and Properties of Friction Surfaced Coatings in AISI 440C Martensitic Stainless Steel," Surf. Coat. Technol., **207**, pp. 310–318.
[109] Nixon, R. G. S., Mohanty, B. S., and Sathish, R., 2018, "Friction Surfacing of AISI 316 Over Mild Steel: A Characteriation Study," Def. Technol., **14**(4), pp. 306–312.
[110] Rafi, H. K., Ram, G. J., Phanikumar, G., and Rao, K. P., 2011, "Microstructural Evolution During Friction Surfacing of Tool Steel H13," Mater. Des., **32**(1), pp. 82–87.
[111] Singh, A. K., Reddy, G. M., and Rao, K. S., 2015, "Pitting Corrosion Resistance and Bond Strength of Stainless Steel Overlay by Friction Surfacing on High Strength Low Alloy Steel," Def. Technol., **11**(3), pp. 299–307.
[112] Rafi, H. K., Phanikumar, G., and Rao, K. P., 2013, "Corrosion Resistance of Friction Surfaced AISI 304 Stainless Steel Coatings," J. Mater. Eng. Perform., **22**(2), pp. 366–370.
[113] Guo, D., Kwok, C. T., Tam, L. M., Zhang, D., and Li, X., 2020, "Hardness, Microstructure and Texture of Friction Surfaced 17–4PH Precipitation Hardening Stainless Steel Coatings With and Without Subsequent Aging," Surf. Coat. Technol., **402**, p. 126302.
[114] Khalid Rafi, H., Janaki Ram, G. D., Phanikumar, G., and Rao, K. P., 2010, "Microstructure and Properties of Friction Surfaced Stainless Steel and Tool Steel Coatings," *Materials Science Forum*, T. Chandra, N. Wanderka, W. Reimers, and M. Ionescu, eds., Trans Tech Publications Ltd, 638–642, pp. 864–869.
[115] Guo, D., Kwok, C. T., and Chan, S. L. I., 2018, "Fabrication of Stainless Steel 316L/TiB_2 Composite Coating via Friction Surfacing," Surf. Coat. Technol., **350**, pp. 936–948.
[116] Kumar, A., and Bauri, R., 2019, "A Novel Method to Process Oxide Dispersed Strengthened Alloy Interconnect," Materialia, **5**, p. 100229.
[117] Kumar, A., and Bauri, R., 2019, "A Novel Thermomechanical Processing Route to Fabricate ODS Ferritic Stainless Steel Interconnects and Their Oxidation Behavior," Oxid. Met., **91**(5–6), pp. 609–624.
[118] Huang, Y., Lv, Z., Wan, L., Shen, J., and dos Santos, J. F., 2017, "A new Method of Hybrid Friction Stir Welding Assisted by Friction Surfacing for Joining Dissimilar Ti/Al Alloy," Mater. Lett., **207**, pp. 172–175.
[119] Fitseva, V., Krohn, H., Hanke, S., and Dos Santos, J. F., 2015, "Friction Surfacing of Ti–6Al–4V: Process Characteristics and Deposition Behaviour at Various Rotational Speeds," Surf. Coat. Technol., **278**, pp. 56–63.
[120] Vale, N., Fitseva, V., Urtiga Filho, S. L., dos Santos, J. F., and Hanke, S., 2019, "Comparison of Friction Surfacing Process and Coating Characteristics of Ti-6Al-4V and Ti Grade 1," JOM, **71**(12), pp. 4339–4348.
[121] Fitseva, V., Hanke, S., dos Santos, J. F., Stemmer, P., and Gleising, B., 2016, "The Role of Process Temperature and Rotational Speed in the Microstructure Evolution of Ti-6Al-4V Friction Surfacing Coatings," Mater. Des., **110**, pp. 112–123.
[122] Dovzhenko, G., Hanke, S., Staron, P., Maawad, E., Schreyer, A., and Horstmann, M., 2018, "Residual Stresses and Fatigue Crack Growth in Friction Surfacing Coated Ti-6Al-4V Sheets," J. Mater. Process. Technol., **262**, pp. 104–110.

[123] Belei, C., Fitseva, V., Dos Santos, J. F., Alcântara, N. G., and Hanke, S., 2017, "TiC Particle Reinforced Ti-6Al-4V Friction Surfacing Coatings," Surf. Coat. Technol., **329**, pp. 163–173.
[124] Hanke, S., Sena, I., Coelho, R. S., and dos Santos, J. F., 2018, "Microstructural Features of Dynamic Recrystallization in Alloy 625 Friction Surfacing Coatings," Mater. Manuf. Processes, **33**(3), pp. 270–276.
[125] Kumar, V. A., and Sammaiah, P., 2018, "Comparison of Process Parameters Influence on Mechanical and Metallurgical Properties of Zinc Coating on Mild Steel and Aluminium During Mechanical Process," Mater. Today: Proc., **5**(2), pp. 3861–3866.
[126] Zhang, G. F., Jiao, W. M., and Zhang, J. X., 2014, "Filling Friction Stir Weld Keyhole Using Pin Free Tool and T Shaped Filler bit," Sci. Technol. Weld. Joining, **19**(2), pp. 98–104.
[127] Jujare, T., Kumar, A., Kailas, S. V., and Bhat, K. U., 2014, "Friction Surfacing of Mild Steel by Copper: A Feasibility Study," Procedia Mater. Sci., **5**, pp. 1300–1307.
[128] Murugan, C. B. K., Balusamy, V., Padmanaban, R., and Vignesh, R. V., 2018, "Friction Surfacing Mild-Steel With Monel and Predicting the Coating Parameters Using Fuzzy Logic," Mater. Today: Proc., **5**(8), pp. 16402–16410.
[129] Rao, K. P., Damodaram, R., Rafi, H. K., Ram, G. J., Reddy, G. M., and Nagalakshmi, R., 2012, "Friction Surfaced Stellite6 Coatings," Mater. Charact., **70**, pp. 111–116.
[130] Hanke, S., Fischer, A., Beyer, M., and Dos Santos, J., 2011, "Cavitation Erosion of NiAl-Bronze Layers Generated by Friction Surfacing," Wear, **273**(1), pp. 32–37.
[131] Hanke, S., Fischer, A., and dos Santos, J. F., 2015, "Sliding Wear Behaviour of a Cr-Base Alloy After Microstructure Alterations Induced by Friction Surfacing," Wear, **338–339**, pp. 332–338.
[132] Nakama, D., Katoh, K., and Tokisue, H., 2008, "Some Characteristics of AZ31/AZ91 Dissimilar Magnesium Alloy Deposit by Friction Surfacing," Mater. Trans., **49**(5), pp. 1137–1141.
[133] Yamashita, Y., and Fujita, K., 2001, "Newly Developed Repairs on Welded Area of LWR Stainless Steel by Friction Surfacing," J. Nucl. Sci. Technol., **38**(10), pp. 896–900.
[134] Liu, X., Yao, J., Wang, X., Zou, Z., and Qu, S., 2009, "Finite Difference Modeling on the Temperature Field of Consumable-Rod in Friction Surfacing," J. Mater. Process. Technol., **209**(3), pp. 1392–1399.
[135] Srivastava, M., Rathee, S., Maheshwari, S., Siddiquee, A. N., and Kundra, T. K., 2019, "A Review on Recent Progress in Solid State Friction Based Metal Additive Manufacturing: Friction Stir Additive Techniques," Crit. Rev. Solid State Mater. Sci., **44**(5), pp. 345–377.
[136] Rathee, S., Srivastava, M., Maheshwari, S., Kundra, T. K., and Siddiquee, A. N., 2018, "Friction Based Additive Manufacturing Technologies: Principles for Building in Solid State," *Benefits, Limitations, and Applications*, 1st ed., CRC Press, Boca Raton, FL.
[137] Palanivel, S., and Mishra, R. S., 2017, "Building Without Melting: A Short Review of Friction-Based Additive Manufacturing Techniques," Int. J. Addit. Subtract. Mater. Manuf., **1**(1), pp. 82–103.
[138] Khodabakhshi, F., and Gerlich, A. P., 2018, "Potentials and Strategies of Solid-State Additive Friction-Stir Manufacturing Technology: A Critical Review," J. Manuf. Process., **36**, pp. 77–92.
[139] Dalgaard, E., Wanjara, P., Gholipour, J., Cao, X., and Jonas, J. J., 2012, "Linear Friction Welding of a Near-β Titanium Alloy," Acta Mater., **60**(2), pp. 770–780.
[140] Dilip, J. J. S., Janaki Ram, G. D., and Stucker, B. E., 2012, "Additive Manufacturing with Friction Welding and Friction Deposition Processes," Int. J. Rapid Manuf., **3**(1), pp. 56–69.
[141] García, A. M. M., 2011, "BLISK Fabrication by Linear Friction Welding," Adv. Gas Turb. Technol., pp. 411–434.
[142] Palanivel, S., Nelaturu, P., Glass, B., and Mishra, R. S., 2015, "Friction Stir Additive Manufacturing for High Structural Performance Through Microstructural Control in an Mg Based WE43 Alloy," Mater. Des., **65**, pp. 934–952.
[143] Yu, H. Z., Jones, M. E., Brady, G. W., Griffiths, R. J., Garcia, D., Rauch, H. A., Cox, C. D., and Hardwick, N., 2018, "Non-Beam-Based Metal Additive Manufacturing Enabled by Additive Friction Stir Deposition," Scr. Mater., **153**, pp. 122–130.
[144] MELD Brochure, 2018, Aeroprobe Corporation, http://www.aeroprobe.com/meld/, Accessed December 28, 2020.
[145] Griffiths, R. J., Perry, M. E. J., Sietins, J. M., Zhu, Y., Hardwick, N., Cox, C. D., Rauch, H. A., and Yu, H. Z., 2019, "A Perspective on Solid-State Additive Manufacturing of Aluminum Matrix Composites Using MELD," J. Mater. Eng. Perform., **28**(2), pp. 648–656.
[146] Garcia, D., Hartley, W. D., Rauch, H. A., Griffiths, R. J., Wang, R., Kong, Z. J., Zhu, Y., and Yu, H. Z., 2020, "In Situ Investigation Into Temperature Evolution and Heat Generation During Additive Friction Stir Deposition: A Comparative Study of Cu and Al-Mg-Si," Addit. Manuf., **34**, p. 101386.
[147] Anderson-Wedge, K., Avery, D. Z., Daniewicz, S. R., Sowards, J. W., Allison, P. G., Jordon, J. B., and Amaro, R. L., 2021, "Characterization of the Fatigue Behavior of Additive Friction Stir-Deposition AA2219," Int. J. Fatigue, **142**, p. 105951.
[148] Rivera, O. G., Allison, P. G., Brewer, L. N., Rodriguez, O. L., Jordon, J. B., Liu, T., Whittington, W. R., Martens, R. L., McClelland, Z., Mason, C. J. T., Garcia, L., Su, J. Q., and Hardwick, N., 2018, "Influence of Texture and Grain Refinement on the Mechanical Behavior of AA2219 Fabricated by High Shear Solid State Material Deposition," Mater. Sci. Eng. A, **724**, pp. 547–558.
[149] Yoder, J. K., Griffiths, R. J., and Yu, H. Z., 2021, "Deformation-Based Additive Manufacturing of 7075 Aluminum With Wrought-Like Mechanical Properties," Mater. Des., **198**, p. 109288.
[150] Griffiths, R. J., Petersen, D. T., Garcia, D., and Yu, H. Z., 2019, "Additive Friction Stir-Enabled Solid-State Additive Manufacturing for the Repair of 7075 Aluminum Alloy," Appl. Sci., **9**(17), p. 3486.
[151] Griffiths, R. J., Garcia, D., Song, J., Vasudevan, V. K., Steiner, M. A., Cai, W., and Yu, H. Z., 2021, "Solid-state Additive Manufacturing of Aluminum and Copper Using Additive Friction Stir Deposition: Process-Microstructure Linkages," Materialia, **15**, p. 100967.
[152] Rutherford, B. A., Avery, D. Z., Phillips, B. J., Rao, H. M., Doherty, K. J., Allison, P. G., Brewer, L. N., and Jordon, J. B., 2020, "Effect of Thermomechanical Processing on Fatigue Behavior in Solid-State Additive Manufacturing of Al-Mg-Si Alloy," Metals, **10**(7), p. 947.
[153] Avery, D. Z., Rivera, O. G., Mason, C. J. T., Phillips, B. J., Jordon, J. B., Su, J., Hardwick, N., and Allison, P. G., 2018, "Fatigue Behavior of Solid-State Additive Manufactured Inconel 625," JOM, **70**(11), pp. 2475–2484.
[154] Rivera, O. G., Allison, P. G., Jordon, J. B., Rodriguez, O. L., Brewer, L. N., McClelland, Z., Whittington, W. R., Francis, D., Su, J., Martens, R. L., and Hardwick, N., 2017, "Microstructures and Mechanical Behavior of Inconel 625 Fabricated by Solid-State Additive Manufacturing," Mater. Sci. Eng. A, **694**, pp. 1–9.
[155] McClelland, Z., Avery, D. Z., Williams, M. B., Mason, C. J. T., Rivera, O. G., Leah, C., Allison, P. G., Jordon, J. B., Martens, R. L., and Hardwick, N., 2019, "Microstructure and Mechanical Properties of High Shear Material Deposition of Rare Earth Magnesium Alloys WE43," *Magnesium Technology*, V. Joshi, J. Jordon, D. Orlov, and N. Neelameggham, eds., The Minerals, Metals & Materials Series, Springer, Cham, pp. 277–282.
[156] Li, B., Shen, Y., Lei, L., and Hu, W., 2014, "Fabrication and Evaluation of Ti3Alp/Ti–6Al–4V Surface Layer via Additive Friction-Stir Processing," Mater. Manuf. Processes, **29**(4), pp. 412–417.
[157] Priedeman, J. L., Phillips, B. J., Lopez, J. J., Tucker Roper, B. E., Hornbuckle, B. C., Darling, K. A., Jordon, J. B., Allison, P. G., and Thompson, G. B., 2020, "Microstructure Development in Additive Friction Stir-Deposited Cu," Metals, **10**(11), p. 1538.
[158] Yu, H. Z., and Mishra, R. S., 2021, "Additive Friction Stir Deposition: A Deformation Processing Route to Metal Additive Manufacturing," Mater. Res. Lett., **9**(2), pp. 71–83.
[159] Jordon, J. B., Allison, P. G., Phillips, B. J., Avery, D. Z., Kinser, R. P., Brewer, L. N., Cox, C., and Doherty, K., 2020, "Direct Recycling of Machine Chips Through a Novel Solid-State Additive Manufacturing Process," Mater. Des., **193**, p. 108850.
[160] Withers, P. J., 2007, "Residual Stress and Its Role in Failure," Rep. Prog. Phys., **70**(12), pp. 2211–2264.
[161] Rathee, S., Maheshwari, S., and Siddiquee, A. N., 2018, "Issues and Strategies in Composite Fabrication via Friction Stir Processing: A Review," Mater. Manuf. Processes, **33**(3), pp. 239–261.